Identification and characterisation of suppressors of synthetic lethality resulting from loss of SETD2 and WEE1

Dissertation submitted for the degree of MSc by Research in Oncology

Department of Oncology, University of Oxford

Linda van Bijsterveldt

Lady Margaret Hall, University of Oxford

Trinity Term 2017

Contents list

Acknowledgements

First and foremost, I would like to thank my supervisor, Associate Professor Timothy Humphrey, for his continuous patience and academic supervision throughout my MSc project. He taught me how to express my ideas and showed me different ways to approach a scientific problem. His enduring enthusiasm for research and his great efforts to explain things clearly and simply, reinforced my desire to pursue a doctorate degree in Oncology at the University of Oxford.

I would also like to thank all past and present members of the Humphrey lab who have helped me along the way, most notably Dr. Sovan Sarkar for his constant technical advice, good company, encouragements and insightful (and challenging) comments on this dissertation. This project has greatly benefited from help from various other people within the CRUK/MRC Oxford Institute for Radiation Oncology. I am very grateful to Dr. Chen-Chun Pai and Dr. Sovan Sarkar for allowing me to use the *S. pombe* suppressor screen data and to Delia Könnig (Eric O'Neill lab), who kindly let me use her OCT4 primers and neural stem cell cDNA.

Outside of science, I would like to thank my Mom and Dad, and my sister, Inge, for boosting my morale with their love, encouragement and constant belief in me. They endured my headstrong ideas on future plans and consistently supported me over the course of my journey towards a Master's degree.

Abstract

Our lab has recently identified a conserved synthetic lethality between loss of SETD2-dependent H3K36 trimethylation and inhibition of WEE1 kinase (Pfister et al., 2015). In order to explore the possible mechanisms of resistance to WEE1 inhibitor-treatment in H3K36me3-deficient cells, a yeast genetic screen was performed to isolate mutants that suppressed the *set2Δ wee1-50* temperature sensitivity. Whole-genome sequencing of 23 spontaneous suppressor mutants revealed mutations in eight genes involved in cell cycle regulation (*bub1, cdc2, cut2, cut1, gtb1, myo52, slp1* and *wee1*), five genes involved in cell communication (*gpa1, shk1, ssp2, ste20* and *wis1*), and seven genes involved in transcription (*bdf1, brf1, bye1, epl1, lsm4, paf1* and *taf10*).

Further analysis in mammalian cells revealed that knockdown of RNA Polymerase II-associated factor 1 (PAF1) partially rescued cell viability at higher concentrations (300 and 600 nM) of the WEE1 inhibitor AZD1775 in both *SETD2* wild-type and *SETD2* CRISPR knockout U2OS cells. Data were verified in fission yeast as well as in the renal cell carcinoma cell lines 786-O (*SETD2* wild-type) and A498 (bearing a truncating mutation in *SETD2*), indicating functional conservation of Paf1/PAF1-dependent resistance to Wee1/WEE1 inhibition from fission yeast to mammalian cells.

Investigations into the molecular mechanisms responsible for PAF1-mediated suppression in human cells suggested involvement of the CDK inhibitor $p21^{Cip1/Waf1}$. Knockdown of PAF1 induced relocalisation of $p21^{Cip1/Waf1}$ to the cytoplasm where it is thought to suppress caspase-3 dependent apoptosis as well as the degradation of RRM2 via CDK2 inhibition in the presence of AZD1775. These findings suggest that targeting cytoplasmic $p21^{Cip1/Waf1}$ may offer new strategies for the treatment of resistance to WEE1-inhibition and knowledge of this pathway should be taken into account in the design of trials of targeted therapies for H3K36me3-deficient cancers.

Abbreviations

ccRCC	Clear cell renal cell carcinoma
CDK	Cyclin-dependent kinase
CKI	Cyclin-dependent kinase inhibitor
CIMP	CpG-island methylator phenotype
CTD	C-terminal domain
DMSO	Dimethyl sulfoxide
DNMT3b	*De novo* DNA methyltransferase b
dNTP	Deoxyribonucleoside triphosphate
DSBs	Double-strand breaks
G418	Geneticin
H3K36me3	Histone H3 lysine 36 trimethylation
hCDK1	Human cyclin-dependent kinase 1
HIF-1α	Alpha subunit of hypoxia-inducible factor 1
HR	Homologous recombination
IC_{50}	Half maximal inhibitory concentration
I_{max} %	Survival rate at maximum inhibition
KO	Knockout
LOH	Loss of heterozygosity
MAP2K1/MEK1	Mitogen-activated protein kinase kinase
NSCs	Neural stem cells
Oct4	Octamer-binding transcription factor 4
PAF1	RNA Polymerase II-associated factor 1

PTMs	Post-translational modifications
Rb	Retinoblastoma susceptibility protein
RCC	Renal cell carcinoma
RNA Pol II	Ribonucleic acid (RNA) Polymerase II
RNR	Ribonucleotide reductase
RRM2	Ribonucleotide reductase regulatory subunit 2
SAC	Spindle assembly checkpoint
SETD2	SET-domain-containing 2
siRNA	Short interfering ribonucleic acids
TAFs	TATA-binding protein associated factors
TSG	Tumour suppressor gene
TSS	Transcription start site
WEE1i	WEE1 inhibition
WT	Wild-type
YE6S	Yeast extract six supplements

List of tables

List of figures

1 Chapter 1: Introduction

1.1 General introduction into renal cancer pathogenesis

1.1.1 Epidemiology and clinical aspects of renal cell carcinoma

Renal cell carcinoma (RCC) encompasses a heterogeneous group of cancers that arise in the renal parenchyma and accounts for 2.4% of all adult malignancies (Ferlay et al., 2013). In 2012, an estimated 340,000 new cases were diagnosed worldwide and this number is only predicted to rise over the next few decades, reflecting an ageing and increasing global population (Ferlay et al., 2013).

RCCs can be further subdivided into 10 histopathological subtypes, with the majority of cases classified as clear cell renal cell carcinoma (ccRCC) or non-papillary RCC (Lopez-Beltran, Scarpelli, Montironi, & Kirkali, 2006). Clear cell RCC originates from mature proximal tubular epithelial cells and comprises approximately 75-80% of all kidney tumours (Lopez-Beltran et al., 2006; Thoenes, Störkel, & Rumpelt, 1986). Clear cell RCC has a worse prognosis compared to other RCC subtypes, such as papillary RCC and chromophobe RCC, and accounts for the majority of deaths from kidney cancer (Capitanio et al., 2009; Keegan et al., 2012).

Surgical resection with curative intent, the "gold standard" management of ccRCC, is only available to patients with limited stage disease (Ljungberg et al., 2015). However, up to one-third of the RCC patients present with locally advanced or metastatic disease at the time of diagnosis (Lam, Leppert, Belldegrun, & Figlin, 2005). Late stage RCCs are notoriously resistant to chemotherapy and none of the conventional cytotoxic chemotherapy agents have demonstrated significant activity, resulting in 5-year survival rates as low as 28% (Mickisch, 1994; Lam *et al*., 2005; Ljungberg *et al.*, 2016).

1.1.2 Molecular pathology of clear cell renal cell carcinoma

Tumour initiation is thought to be the result of a genetic alteration in the genome of a somatic cell, leading to abnormal behaviour and proliferation of the cell in which the mutation occurs (Cooper & Hausman, 2007). Through repeated cycles of cell growth and division, this subsequently leads to the outgrowth of a population of clonally-derived tumour cells. Tumour progression continues as recessive loss-of-function mutations in tumour suppressor genes (TSGs) confer a selective advantage to the tumour population (Cooper & Hausman, 2007).

Clear cell RCC has long been considered a cancer initiated by inactivation of the TSG *VHL* (Cancer Genome Atlas Research Network, 2013). Upon exposure of cells to normal oxygen tension, pVHL mediates ubiquitination and subsequent proteosomal degradation of the alpha subunit of the hypoxia-inducible factor 1 (HIF-1α) (Maxwell et al., 1999). Bi-allelic loss of *VHL* in ccRCC is sufficient to dysregulate ubiquitin-dependent proteolysis of HIF-1α and can therefore cause accumulation of HIF-1α within the nucleus. Nuclear HIF-1α promotes transcription of a set of hypoxia responsive genes, including pro-tumourigenic genes such as vascular endothelial growth factor (VEGF) and the platelet-derived growth factor B chain (PDGFB) (Iliopoulos, Levy, Jiang, Kaelin, & Goldberg, 1996). Subsequent binding of VEGF to its receptor (VEGFR) leads to phosphorylation of downstream kinases and activation of the RAF1-MEK-ERK1/2 and PI3K-AKT-mTOR pathways (reviewed in Simons *et al.* 2016).

The *VHL* gene is located at the 3p25 locus and inactivation of this gene is caused by single copy loss of 3p (Latif et al., 1993). Loss of heterozygosity (LOH) at the short arm of chromosome 3 is the most frequent genetic aberration in ccRCC and occurs in about 91% of all kidney carcinomas (Cancer Genome Atlas Research Network, 2013). Numerous lines of evidence have however indicated that loss of *VHL* is insufficient to cause tumourigenesis and its relationship to adverse tumour features and negative clinical outcomes has thus far been conflicting (Martinez et al., 2000; Sato et al., 2013).

Recent large-scale sequencing projects have revealed that LOH of 3p results in inactivation of additional TSGs besides *VHL*, most of them residing in close proximity to the 3p21 locus (Hakimi, Chen, et al., 2013). These TSGs have recently been identified as *PBRM1*, *SETD2*, and *BAP1* and were found to be mutated in respectively 29.2%, 7.6%, and 6.9% of ccRCCs (Hakimi, Chen, et al., 2013). Interestingly, all three genes are known to have an important role in epigenetic control of gene expression and the above-mentioned findings have therefore generated the hypothesis that epigenetic reprogramming, resulting from the disruption of chromatin remodelling machinery, plays a fundamental role in the development and pathogenesis of ccRCC following loss of *VHL* (Cancer Genome Atlas Research Network, 2013; Dalgliesh et al., 2010; Hakimi, Chen, et al., 2013).

1.1.3 SETD2 and cancer

According to the Catalogue of Somatic Mutations in Cancer (COSMIC) database, *SETD2* (11%) is ranked fourth in the top-20 most commonly mutated genes in ccRCC, only preceded by *VHL* (46%), *PBRM1* (31%), and *BAP1* (12%) (http://cancer.sanger.ac.uk/cosmic). Although under-expression and mutation of *SETD2* is most commonly found in kidney cancer, mutations in *SETD2* have also been reported in a wide range of other tumour types (Cancer Genome Atlas Research Network, 2013; Duns et al., 2010) (*Table 1.1*), supporting an important role for SETD2 as tumour suppressor in diverse malignancies.

Table 1.1. *Overview of SETD2 mutation frequencies in a selection of tumours. Source: COSMIC database (July 2017).*

Tissue	*SETD2* mutation (%)
Kidney	7.72
Skin	5.12
Soft tissue	4.01
Endometrium	3.75
Large intestine	3.61
Liver	2.53
Stomach	2.41

In mammalian cells, the tumour suppressor SET-domain-containing 2 (SETD2) is the sole histone methyltransferase responsible for adding a methyl group to a di-methylated lysine to generate a trimethyl mark (H3K36me3) (Edmunds, Mahadevan, & Clayton, 2008). Consequently, tumour cells bearing frameshift or missense mutations in *SETD2* (*Figure 1.1*) completely lack trimethylated H3K36me3 (Gerlinger et al., 2012).

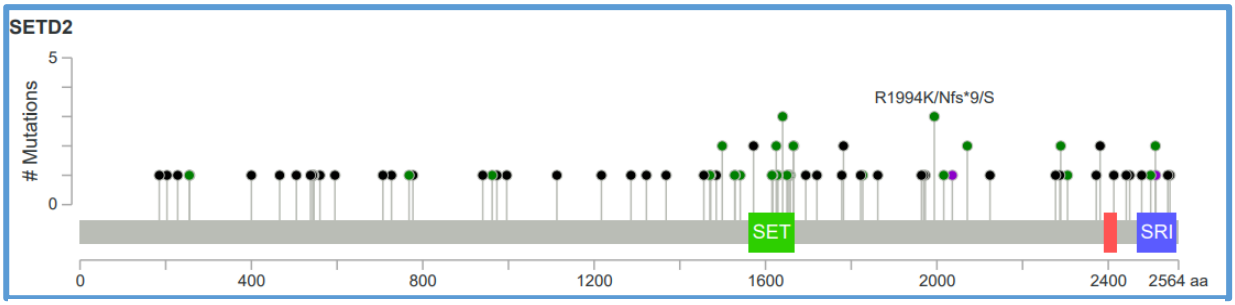

Figure 1.1. Distribution of mutations in clear cell renal cell carcinoma with respect to the key functional domains of human SETD2. *Coloured regions in protein diagram represent protein domains (lime green, SET domain; red, WW domain; pink, purple, SRI [Set2 Rpbl-interacting] domain). Mutation diagram circles are coloured with respect to the corresponding mutation types; missense mutation (green), truncating mutation (black) and other mutations (purple). From:* http://cancer.sanger.ac.uk/cosmic.

A recent study using multi-region exome sequencing has identified considerable intratumoural heterogeneity within primary ccRCCs (Ricketts & Linehan, 2014) and consequently, H3K36me3 levels are only significantly reduced in a subset (~20%) of primary ccRCC tumour cells (Ho et al., 2015). Notably, however, H3K36me3-positive nuclei are further reduced in metastatic ccRCC (with 60%), indicating that SETD2 methyltransferase activity is progressively impeded during RCC tumour progression (Ho et al., 2015).

For the reason that biallelic *SETD2* inactivation and subsequent loss of the epigenetic mark H3K36me3 have been associated with more advanced disease state and reduced cancer-specific survival (Hakimi, Ostrovnaya, et al., 2013), there has been increased interest in developing therapeutic strategies targeting H3K36me3-deficient cancers. Before providing details on the possibility to target loss of H3K36me3 with the WEE1 inhibitor AZD1775 (Pfister et al., 2015), the domains and functions of SETD2 will be discussed, as well as the role of chromatin dynamics in transcriptional regulation.

1.2 SETD2: an epigenetic modifier with tumour suppressor functionality

1.2.1 Structure of the human methyltransferase SETD2

The human SETD2 protein consists of 2,564 amino acids and has a predicted molecular weight of 287.5 kDa. To date, three conserved functional domains have been identified in SETD2, including a tryptophan (WW) domain (pink), a Set2 Rpb1 interacting domain (blue) and the Set2 domain itself, which consists of the associated with SET (AWS), SET and Post-SET motifs (green) (*Figure 1.1*) (Edmunds et al., 2008; Rebehmed, Revy, Faure, De Villartay, & Callebaut, 2014).

The SET domain is a sequence of 130 amino acids, originally named after the Drosophila genes **S**uppressor of Variegation, **E**nhancer of Zeste and **T**rithorax (Jenuwein, Laible, Dorn, & Reuter, 1998). By virtue of its catalytic SET domain, SETD2 transfers a methyl group from S-adenosyl-L-methionine to the lysine 36 residue of the histone H3 tail (H3K36) (Edmunds et al., 2008).

The Set2 Rpb1 interacting (SRI) domain is highly conserved from yeast to humans (Rebehmed et al., 2014) and preferentially binds the elongating form of RNA polymerase II (RNA Pol II), as revealed by its high affinity to both the serine 2- and serine 5-phosphorylated C-terminal domain (CTD) tail of the largest Rpb1 subunit of RNA Pol II (Kizer et al., 2005; B. Li, Howe, Anderson, Yates, & Workman, 2003). Accordingly, transcription rates positively correlate with SETD2 recruitment in higher eukaryotes, resulting in higher levels of H3K36me3 downstream of the first exons of actively transcribed genes (Bannister et al., 2005; B. Li et al., 2003; Shilatifard, 2006).

WW domains are present in many human proteins and are thought to mediate a wide variety of biological functions, including RNA Pol II activity, owing to their ability to recognize proline-rich sequences (Sudol, Sliwa, & Russo, 2001).

1.2.2 From structure to biological function: H3K36me3 and transcriptional regulation

The above-mentioned functional domains define the best-understood biological function of SETD2, which is co-transcriptional catalysis of H3K36 trimethylation via its association with RNA Pol II. Many of the more recent research efforts have been addressing the question of how specific histone post-translational modifications (PTMs) are coordinated with elongating RNA Pol II, and how this pattern can then affect gene expression. In this subsequent section, the role of chromatin in transcriptional regulation will be explained in more detail, as well as the role of "reader" complexes that are responsible for histone PTM pattern recognition and "translate" the PTMs by carrying out distinct cellular processes.

1.2.2.1 Basic organisation of chromatin

The genomic DNA of eukaryotic cells is highly folded and compacted into condensed chromatin (Horn & Peterson, 2002). Nucleosomes, the repeating unit of chromatin, are composed of two copies of each of the four highly conserved alkaline core histones (H2A, H2B, H3 and H4) wrapped by approximately 147 base pairs of double-stranded DNA (Horn & Peterson, 2002; Luger, Mäder, Richmond, Sargent, & Richmond, 1997). Eight highly positively charged *N*-terminal tails are protruding from the flat surface of the histone octamer and allow for the formation of inter-particle connections, i.e. attachments to the DNA or acidic histone domains of neighbouring nucleosomes (Arya & Schlick, 2009).

Eukaryotic chromatin is in equilibrium between two higher order structures: active euchromatin and silent heterochromatin, depending on its level of compaction (Horvath,

Bailey, Locke, & Eichler, 2001). As the variation in packing density allows for differences in the accessibility of transcription start sites (TSS) to transcription factors and RNA Pol II, chromatin reconfiguration can alter expression of genes and other genetic elements (Horn & Peterson, 2002; Jiang & Pugh, 2009).

Chromatin structure and function are regulated by several mechanisms, including chromatin remodelling, the incorporation of histone variants, and histone modification. As a review of all these regulatory mechanism is beyond the scope of this dissertation, focus will be kept on the covalent post-translational modifications (PTMs) of histones.

1.2.2.2. Regulation of chromatin structure by histone methylation

The majority of PTMs localise to amino acid residues in the *N*-terminal tail of histones and regularly consist of ubiquitination, serine phosphorylation, and methylation and acetylation of lysine or arginine residues (Ruthenburg, Li, Patel, & David Allis, 2007). Modifications on the *N*-terminal tails can alter chromatin compaction by disrupting DNA-histone interactions as well as affect the recruitment of enzyme reader complexes that regulate a wide variety of biological processes (Arya & Schlick, 2009).

Two of the most well characterised histone modifications include methylation of lysine (K) and arginine (R) residues of histone H3 or H4. The addition or removal of methyl groups from histone tails is regulated by the action of enzymes with opposing functions, called methyltransferases (writers) and demethylases (erasers). Lysine methyltransferases work through the transfer of a S-adenosyl-L-methionine group to the ε-nitrogen of the target lysine residue, generating mono-, di- or tri-methylated states (me1, me2 and me3, respectively) (reviewed in Smith and Denu, 2009). PTMs have previously been found to be highly specific with regard to a specific state of methylation and the K residue on which they operate in the nucleus of eukaryotic cells, owing to their ability to discriminate between different amino

acid sequences surrounding the target residue (Edmunds et al., 2008). Although yeast homolog Set2 is responsible for mono-, di- and trimethylation of the Lys36 residue (Strahl et al., 2002), the human SETD2 protein was found to be exclusively responsible for adding a methyl group to a di-methylated lysine (Edmunds et al., 2008).

Addition or removal of a methyl group does not alter the charge of the amino acid side chain and its function is therefore thought to be predominantly mediated by recruitment of so-called 'reader' complexes that contain a methyl-lysine-binding motif (reviewed in Musselman et al. 2014). Several lysine methylation 'reader' complexes have been identified so far, including ankyrin-, bromo adjacent homology (BAH)-, chromo-, HEAT-, malignant brain tumour (MBT)-, plant homeodomain (PHD)-, PWWP-, Tudor-, WD40- and zinc finger CW-domains (reviewed in Musselman *et al.* 2014). Those 'reader' complexes, together with their target methyl-lysines, can assist in the targeting of co-factors and other complexes to modified chromatin and thus determine the functional outcome of lysine methylations.

Methylation of a lysine residue may thus lead to formation of either heterochromatin or euchromatin, depending on the methylation state of the modified residue (Black, Van Rechem, & Whetstine, 2012). Generally, H3K4 and H3K36 trimethylations are associated with euchromatin, whereas H3K9, H3K27 and H3K79 trimethylations are considered to mark heterochromatin (Black et al., 2012).

1.2.3 Other H3K36me3-mediated biological functions

As discussed in *Chapter 1.2.1* and *1.2.2*, one of the most important functions of SETD2 is to modulate chromatin structure during transcriptional elongation via its association with serine 2-phosphorylated RNA Pol II (Sun et al., 2005; Yoh, Lucas, & Jones, 2008). The epigenetic mark H3K36me3 however also mediates some other important processes in human cells,

including DNA methylation and cryptic transcription, DNA repair (Aymard et al., 2014; Pfister et al., 2014), and pre-mRNA splicing (Sorenson et al., 2016).

Roles for SETD2-dependent trimethylation of histone H3K36 in maintaining genomic integrity, a hallmark of cancer, have only recently been discovered. H3K36me3 regulates DNA mismatch repair in human cells by recruiting the mismatch recognition protein hMutSα onto chromatin through direct interactions with its PWWP domain (F. Li et al., 2013). H3K36me3 is also a crucial factor in the repair of DNA double-strand breaks (DSBs) in transcriptionally active chromatin, via a repair pathway called homologous recombination (HR) (Aymard et al., 2014; Pfister et al., 2014). When H3K36me3 is abolished due to inactivation of *SETD2,* binding of Lens Epithelium Derived Growth Factor (LEDGF) – also referred to as p75 – to damage sites is prevented (Pfister et al., 2014). Reduced levels of LEDGF lead to impaired recruitment of the C-terminal binding protein interacting protein (CtIP) to DNA DSBs and subsequent defects in DNA-end resection (Daugaard et al., 2012; Pfister et al., 2014). DSBs that have not been resected cannot rely on HR for efficient repair and cells thus have to use alternative, and often more error-prone mechanisms of repair, such as non-homologous end-joining (NHEJ) and/or microhomology-mediated end-joining (Pfister et al., 2014). Furthermore, loss of H3K36me3 has been proposed to disable the G_1/S-checkpoint, ultimately leading to genomic instability (Carvalho et al., 2014).

SETD2 does not only play an important role in maintaining genome integrity via regulation of DNA damage repair, but also through regulation of DNA methylation. The epigenetic mark H3K36me3 was found to be responsible for binding of the PWWP domain of *de novo* DNA methyltransferase b (DNMT3b), which can establish genomic DNA methylation on cytosine residues in CpG-dense regions within gene bodies (Baubec et al., 2015). In the absence of SETD2, DNMT3b-dependent DNA methylation is not properly targeted to actively transcribed regions, leading to aberrant transcription initiation events from cryptic

promoter-like sequences within the 3' region of gene bodies (Neri et al., 2017). Comprehensive genome-wide studies in human cells have confirmed a role for SETD2 in preventing spurious transcription initiation, as downregulation of SETD2 resulted in an increase in RNA Pol II occupancy at intragenic sites, causing the formation of poly(A)$^+$ transcripts in at least 11% of all active genes (Carvalho et al., 2013). As the formation of cryptic transcripts could lead to inhibition of transcription as well as the production of cryptic proteins, intragenic hypomethylation resulting from loss of SETD2 provides yet another mechanism that could lead to carcinogenesis.

Finally, H3K36me3 has also been associated with regulation of (alternative) mRNA splicing (Sorenson et al., 2016). Recent studies have revealed that exons are preferentially enriched with the epigenetic mark H3K36me3 relative to introns (Kolasinska-Zwierz et al., 2009). Also, H3K36me3 appears to be associated with constitutive exons rather than alternative exons, suggesting a role for H3K36me3 in facilitating exon definition through recruitment of the splicing regulator polypyrimidine tract-binding protein (PTB) via the chromatin binding MORF-related gene (MRG15) (Kolasinska-Zwierz et al., 2009; Luco et al., 2010). Interestingly, it was also shown that efficient and correct splicing was dependent on association of Set2 with the CTD of RNA Pol II through its SRI domain in *S. cerevisiae*, suggesting that Set2 may act co-transcriptionally to recruit splicing factors (Sorenson et al., 2016). Deletion of SETD2 resulted in reduced splicing efficiency across the genome, mainly due to endogenous intron retention and aberrant splicing of genes (Sorenson et al., 2016).

1.3 Cell cycle regulation

Proliferation depends on progression through four distinct cell cycle phases – Gap 1 (G_1), DNA synthesis (S), Gap 2 (G_2), and Mitosis (M) (Mitchison, 1971; Howard and Pelc, 1953). Eukaryotes have an additional gap phase (G_0) in which cells go into a state of quiescence. G_1, S and G_2 are together referred to as interphase, i.e. the time between mitoses, which is when the in S-phase duplicated chromosomes get segregated and the cell divides into two daughter cells (Mitchison, 1971).

1.3.1 Cyclins and cyclin dependent kinases

In eukaryotes, progression through the cell cycle is tightly regulated by correct assembly and activation of cyclin dependent serine/threonine kinases (CDKs) (Cooper & Hausman, 2007). To date, a large number of CDKs have been identified and of these, at least five play an important role in cell cycle regulation. CDK2, CDK4 and CDK6 are active during $G_{0/1}$-phase, CDK2 during S-phase, and CDK1 during mitosis (*Figure 1.2*) (Harper & Brooks, 2004; van den Heuvel & Harlow, 1993). The CDK subunit on its own has no detectable kinase activity and therefore requires binding of positive regulatory subunits known as cyclins (Morgan, 1995; J Pines, 1995).

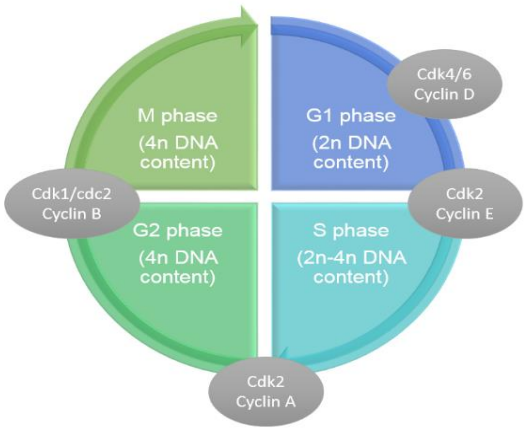

Figure 1.2. Overview of cell cycle regulation in eukaryotes. *According to the classical model of cell cycle control, D-type cyclins and CDK4 or CDK6 regulate events in early G_1 phase, cyclin E-CDK2 triggers S-phase, cyclin A-CDK2 regulates the completion of S-phase, and CDK1-cyclin B is responsible for mitosis.*

The accumulation of cyclins is tightly controlled by elaborate transcriptional networks, as well as by post-translational control through localisation and degradation by ubiquitin-dependent proteolysis. Different cyclins are therefore present at specific phases in the cell cycle and regulate CDK activity in a timely manner (Harper and Brooks, 2004).

Following activation, CDKs can regulate downstream pathways and processes by phosphorylating a large number of substrates, including lamins, histones and other cell cycle proteins (J Pines, 1995). These phosphorylation events regulate the order of events in the cell cycle and transition into the next phase of the cell cycle at several key "checkpoints", including the G_1/S, intra-S, G_2/M, and intra-M checkpoints (Hartwell & Weinert, 1989).

The primary checkpoint acts in mid-to-late G_1-phase and is known as the restriction point (R) (Pardee, 1974). Following passage of the restriction point, cells are committed to the mitotic cell cycle. The main function of the two other checkpoints, in S-phase and at the G_2/M transition, is to block cell cycle progression in response to possible defects during DNA synthesis and chromosome segregation, allowing time for DNA repair to ensure genome integrity (Otto & Sicinski, 2017). The main DNA damage response pathways are mediated via the sensors Ataxia Telangiectasia Mutant (ATM) and ATM and Rad3-related (ATR) and their downstream targets checkpoint kinases 1 (Chk1) and 2 (Chk2) (for a review of the DNA damage checkpoints, see Blackford and Jackson, 2017). The remaining intra-M checkpoint, also known as the spindle assembly checkpoint (SAC), ensures that chromosomes become correctly attached to the microtubule spindle apparatus via their kinetochores (reviewed in Lara-Gonzalez, Westhorpe and Taylor, 2012).

The importance of cell cycle checkpoints for proper cell division and DNA replication is illustrated by the high frequency of mutations that affect checkpoint control in tumourigenesis. Those mutations often lead to unscheduled proliferation and replicative

immortality, one of the hallmarks of cancer cells as proposed by Hanahan and Weinberg (D Hanahan & Weinberg, 2000).

1.3.2 G_0 to G_1 phase transition

Although some cells remain in the non-dividing G_0-phase for the full duration of their lifetime, most cells have the ability to re-enter the cell cycle in G_1 in response to stimulation by external growth factors. As cells enter the cycle from quiescence (G_0), one or more D-type cyclins (D1, D2 and D3) are transcriptionally induced (Baldin, Lukas, Marcote, Pagano, & Draetta, 1993; Inaba et al., 1992; Motokura, Keyomarsi, Kronenberg, & Arnold, 1992) and stabilised via signalling pathways such as the mitogen-activated protein kinase (MAPK) pathway (Aktas, Cai, & Cooper, 1997). The three D-type cyclins preferentially bind with and activate their catalytic partners CDK4 and CDK6 (Matsushime et al., 1994; Meyerson & Harlow, 1994). Cyclin D-CDK4/6 complexes subsequently help to target the retinoblastoma susceptibility protein (Rb) for mono-phosphorylation through direct protein-protein interactions, contributing to increased cellular metabolism (Ewen *et al.*, 1993; Narasimha *et al., 2014*).

1.3.3 G_1 to S-phase transition

At the late G1 restriction point, cyclin E associates with CDK2 and this complex then drives the progression from G_1 into S-phase by completing Rb phosphorylation (Harbour, Luo, Dei Santi, Postigo, & Dean, 1999; Lundberg & Weinberg, 1998; Pagano et al., 1993). Rb hyper-phosphorylation leads to release of the transcription factors E2F-1, E2F-2 and E2F-3 and permits E2F-mediated transcription of a number of S-phase promoting genes, including the

E-type cyclins (E1 and E2) and genes involved in nucleotide metabolism and DNA synthesis (Geng et al., 1996; Johnson & Schneider-Broussard, 1998).

Entry into S-phase can be further regulated by two families of cell cycle inhibitory proteins, called CDK inhibitors (CKIs) (Sherr & Roberts, 1995). The inhibitor of kinase 4 (INK4) family, comprising INK4A (p16), INK4B (p15), INK4C (p18), INK4D (p19), can specifically inhibit CDK4 and CDK6 in early G_1, thereby preventing formation of the CDK4/6-cyclin D complex and subsequent release of the E2F transcription factors (reviewed in Ortega, Malumbres and Barbacid, 2002). The second family, called the CDK interacting protein/kinase inhibitory protein (Cip/Kip) family, includes p21 (Cip1 Waf1), p27 (Cip2), and p57 (Kip2), and is responsible for modulation of activity of various CDK-cyclin complexes, including CDK2-cyclin E (reviewed in Besson *et al.* 2008). The CKI $p21^{Cip1/Waf1}$ is induced by transcriptional activation of tumour suppressor p53 upon DNA damage and is particularly important in mediating G_1 arrest (Sherr & Roberts, 1995).

1.3.4 S-phase

During the S-phase of the cell cycle, the DNA is replicated in order to prepare the cell for division. Activation of CDK4/6-cyclin D just before the onset of S-phase is helping the cell prepare for DNA replication by stimulating assembly of the pre-replicative initiation complex in cooperation with cell division cycle 6 (Cdc6) and proliferating cell nuclear antigen (PCNA) (Coverley, Laman, & Laskey, 2002; Braden *et al*, 2008). As cyclin E1 expression at the G_1/S boundary is accompanied by high E2F1 expression levels, many DNA metabolism genes, including the ribonucleotide reductase regulatory subunit 2 (RRM2), are induced at the beginning of S-phase (Whitfield, 2002)

In the later stages of S-phase, cyclin E is slowly degraded and CDK2 binds another cyclin to form the CDK2-cyclin A complex. The CDK2-cyclin A complex has several functions, including activation of DNA synthesis by recruitment of a number of replication factors, such as Cdc45. Cdc45 recruits DNA polymerase α into pre-replicative initiation complexes, thereby facilitating new origin firing (Coverley et al., 2002).

1.3.5 G_2-phase to mitosis transition and the role of WEE1 kinase

Mitotic onset and the centrosome cycle are regulated by cyclin A and B in complex with CDK1 (King et al. 1994; Arellano & Moreno 1997). Synthesis of cyclin B1, which is thought to be primarily responsible for binding of CDK1, is initiated at the end of S-phase (Jonathon Pines & Hunter, 1989). As is the case with most CDK-cyclin complexes, activation of the CDK1-cyclin B complex is tightly regulated by (de)phosphorylation events, predominantly via the CDC25/WEE1 regulatory pathway (Coleman & Dunphy, 1994). WEE1 activation prevents progression into mitosis by catalysing inhibitory tyrosine-15 phosphorylation in the ATP-binding domain of CDK1 and CDK2, rendering those CDKs inactive. This inhibition can be reversed by CDC25, the human protein responsible for dephosphorylation of tyrosine-15 (Parker & Piwnica-Worms, 1992).

More recent studies, however, have also revealed an important role for WEE1 kinase in regulation of CDK activity during S-phase (Beck et al., 2012). Following WEE1 inhibition in mammalian cells, inhibitory tyrosine-15 phosphorylation on CDK1 and CDK2 was reduced, which resulted in hyper activation of CDK1 and CDK2 during S-phase (Beck et al., 2012). Hyperactive CDK1/2 could thereafter induce replication stress through a rapid increase in origin firing, thereby causing exhaustion of the nucleotide pools (Beck et al., 2012). Imbalance in deoxynucleoside triphosphate (dNTP) pools has a marked impact on fork

progression and results in dysfunctional DNA replication (Beck et al., 2012; Pfister et al., 2015). Additional studies in fission yeast have recently confirmed those findings (Anda *et al.*, 2016; our unpublished results), supporting an evolutionary conserved role for WEE1 in preventing DNA damage via regulation of origin firing (Beck et al., 2012).

During the past decade, several WEE1 inhibitors have been developed pre-clinically (reviewed in Matheson, Backos and Reigan, 2016) and recently, the potent WEE1-inhibitor AZD1775 (also known as MK-1775) has advanced into Phase II clinical studies (http://www.clinicaltrials.gov).

1.3.6 Mitosis and the spindle assembly checkpoint

Following passage of the G_2/M-checkpoint, cells enter mitosis where they undergo cell division. Progression through mitosis is safeguarded by the SAC, which prevents anaphase initiation in the presence of unattached or improperly attached chromosomes to spindle microtubules (Lara-Gonzalez et al., 2012).

1.4 Synthetic lethality resulting from loss of SETD2 and WEE1

1.4.1 General introduction into the concept of synthetic lethality

Two genes or pathways are synthetic lethal if a single mutation in *A* or *B* alone is compatible with cell viability, but inactivation of both *A* and *B* results in cell death (reviewed in Guarente 1993). Genes that interact in this fashion usually function in parallel pathways that are together essential for survival (reviewed in Guarente 1993). Those parallel pathways can either together impinge on an essential biological pathway (e.g. when cancers arising from loss of one DNA repair pathway (e.g. HR) become fully dependent on the other repair pathway (e.g. NHEJ) to survive and defects in both pathways leads to lethality), or those pathways can be totally distinct (e.g. when defects in DNA replication causes generation of DNA damage requiring specific repair pathways, but a second gene defect leading to loss of those repair pathways will cause lethality) (reviewed in Sajesh, Guppy and McManus, 2013).

Identification of those gene-gene synthetic lethal interactions specific for tumour cells, provides a novel angle for human cancer therapy. Synthetic genetic approaches seek to exploit the aberrant genetics (e.g. gene mutation, deletion of amplification) associated with cancer development by targeting a second (unlinked) gene partner with a drug. This approach is therapeutically advantageous to targeting of cancer cells with standard agents, in that their enhanced selectivity towards tumours cells can limit cytotoxic side effects.

The first drug-gene synthetic lethal interaction that has been identified – and recently also approved by the FDA – is where tumours defective in the DNA repair genes *BRCA1* or *BRCA2* can be selectively targeted with Poly (ADP-ribose) polymerase (PARP) inhibitors, owing to their defect in HR (Ashworth, 2008; Bryant et al., 2005; Farmer et al., 2005). Since then, a number of other drug-gene synthetic lethal interactions that can be exploited for human cancer treatment have been discovered.

1.4.2 Mechanism of synthetic lethality resulting from loss of SETD2 and WEE1

Our lab has recently demonstrated that H3K36me3-deficient cancers can be targeted by exploiting a synthetic lethal interaction with WEE1 inhibition (WEE1i) by AZD1775 (MK-1775). Cancer-specific cell death following WEE1 inhibition is thought to occur as a result of persistent replication stress, ultimately leading to replication fork collapse and catastrophe during S-phase (Pfister et al., 2015).

It was found that downregulation of RRM2, the regulatory subunit of the enzyme ribonucleotide reductase (RNR), is required to manifest this synthetic lethality (Pfister et al., 2015). RNR catalyses the rate-limiting step of the formation of deoxyribonucleotides, the precursors of DNA synthesis, by direct reduction of the corresponding ribonucleotides (Elledge, Zhou, & Allen, 1992). RNR genes are cell-cycle regulated and transcription of RRM2 was found to be induced in late G1 and early S phase, directly preceding the initiation of DNA replication (Elledge et al., 1992).

In the context of synthetic lethality resulting from loss of SETD2 and WEE1, RRM2 is regulated via two different pathways (*Figure 1.2*).

1.4.2.1 First pathway: loss of SETD2 leads to reduced RRM2 expression

Because the H3K36me3 chromatin signature is highly coordinated by phosphorylation states of the CTD of RNA Pol II, H3K36me3 is often found enriched at promoters and gene bodies of actively transcribed genes (as discussed in *Chapter 1.2.3*). Chromatin immunoprecipitation followed by real-time quantitative polymerase chain reaction revealed that H3K36me3 was also present at the *RRM2* promoter, where it was responsible for recruitment of multiple TAFs that facilitate transcription initiation (Pfister et al., 2015).

For this reason, reduced methylation state of the epigenetic mark H3K36 following SETD2 depletion causes a reduction in Ser-2 and Ser-5 phosphorylation of the CTD of RNA Pol II as well as a decrease in the total occupancy of RNA Pol II throughout the gene body of *RRM2* (Pfister et al., 2015). Loss of H3K36me3 thus results in inhibition *RRM2* expression via repression of RNA Pol II transcriptional activity (Pfister et al., 2015).

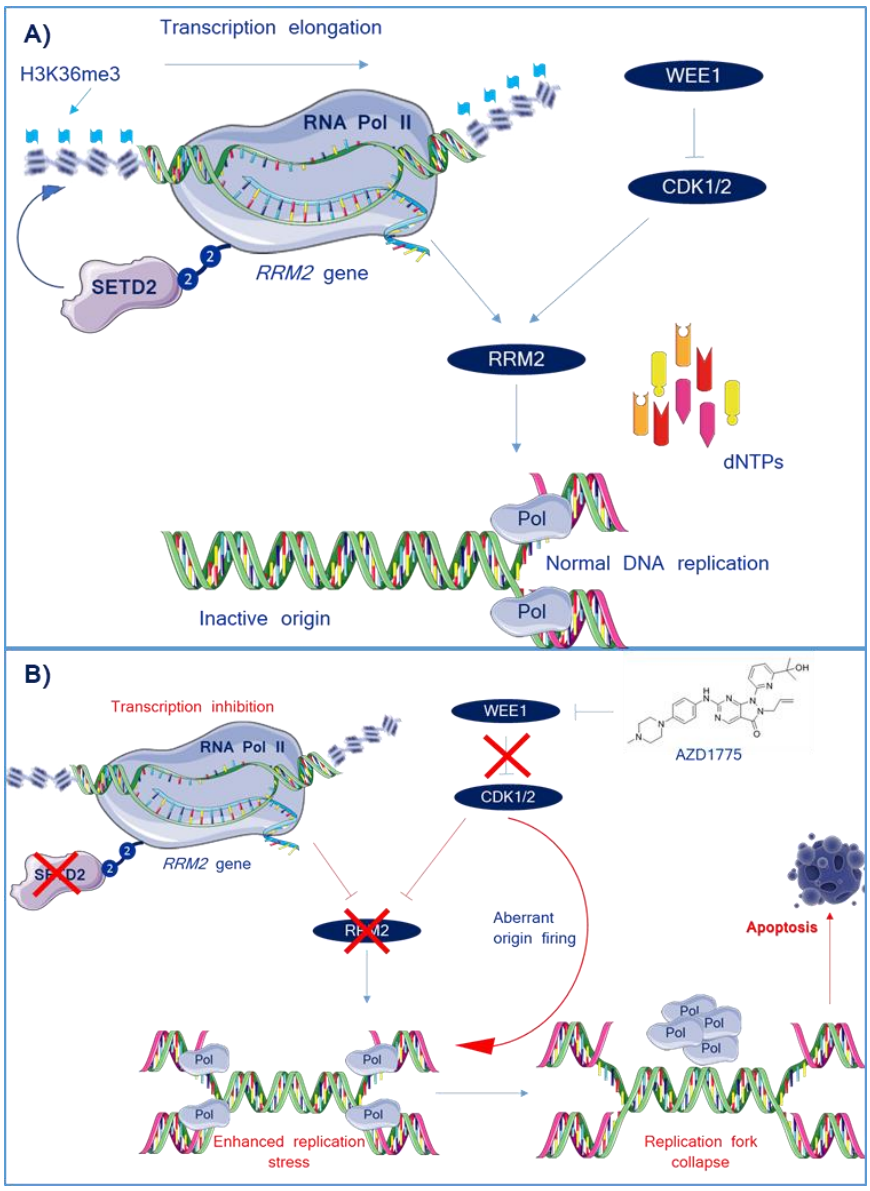

Figure 1.2. Systematic overview of the synthetic lethality resulting from loss of H3K36me3 and WEE1. ***A)*** *In normal cells, RRM2 levels are transcriptionally regulated by SETD2-dependent H3K36 trimethylation and post-transcriptionally by WEE1-dependent inhibition of CDK1/2 activity.* ***B)*** *In cancer cells that have lost H3K36me3, RRM2 transcriptional activity is severely repressed, leading to low dNTP levels. In this background, WEE1 inhibition by AZD1775 further depletes nucleotide pools via CDK1/2-induced RRM2 degradation and increased origin firing. This ultimately leads to DNA replication stress, fork collapse and replicative catastrophe.*

1.4.2.2 Second pathway: inhibition of WEE1 induces aberrant origin firing and RRM2 degradation

Besides a role for WEE1 inhibition in regulating origin firing (as discussed in *Chapter 1.3.4)*, there has also been evidence that WEE1 kinase mediates stability of RRM2. Hyper activation of CDK1/2 leads to an increase in phosphorylation of RRM2 at threonine 33 (D'Angiolella et al., 2012). Phosphorylation of RRM2 at Thr33 exposes the CY motif (residues 49-51 of RRM2) for Cyclin F recognition, thereby promoting RRM2 ubiquitination and degradation via $SCF^{Cyclin\ F}$(D'Angiolella et al., 2012; Pfister et al., 2015). WEE1 inhibition can therefore promote RRM2 degradation via CDK1/2 hyperactivation, thus providing two mechanisms by which it can lower dNTP levels, including aberrant origin firing and RRM2 proteolysis (Pfister et al., 2015).

1.4.2.3 Synthetic lethality resulting from nucleotide depletion and replication fork collapse

Accurate replication of the genome during S-phase is dependent on a constant supply of dNTPs, which is mainly coordinated by tight regulation of RNR activity during G_1 and S-phase (Elledge et al., 1992). Reduced or imbalanced intracellular dNTP pools can impede replication fork progression and cause a reduction in origin usage, thereby inducing replication stress (Poli et al., 2012). Despite the complex responses initiated by the cell to stabilise and restart stalled replication forks, persistent replication stress can provoke catastrophic widespread fork collapse (reviewed in Zeman and Cimprich, 2014). Fork collapse involves dissociation of the replisome and the formation of a DNA DSB at the site of the stalled replication fork (Shimura et al., 2008).

In the context of the synthetic lethality resulting from loss of SETD2 and WEE1, Pfister *et al.* found that addition of AZD1775 to SETD2-deficient cells causes stalled replication forks to

collapse into transient DSBs (Pfister et al., 2015). It is thought that this process is partially mediated by a Mus81, an endonuclease that cleaves branched DNA substrates (Pfister et al., 2015). As the rate of DSB formation at collapsed replication forks exceeds the capacity of SETD2-deficient cells to repair its lesions in the presence of AZD1775, the DNA damage checkpoint is activated and caspase-3-dependent apoptosis is induced (Pfister et al., 2015).

In summary, simultaneous disruption of both pathways – loss of SETD2 (see *Chapter 1.4.2.1*) and inhibition of WEE1 (see *Chapter 1.4.2.2*) - leads to critically low levels of RRM2, followed by S-phase arrest and depletion of dNTP pools (Pfister et al., 2015) (*Figure 1.2*).

1.5 Mechanisms of resistance to AZD1775 treatment in SETD2-deficient cancers

The observations discussed in *Chapter 1.4* have led to assessment of the WEE1 inhibitor AZD1775 as a targeted therapy for SETD2 mutation carriers in several tumour types (http://www.clinicaltrials.gov). Synthetic-lethality based cancer therapies have been proven to be highly effective, but therapy outcomes may not be durable due to recurrent patterns of resistance development within tumours.

Due to genomic instability and selective evolutionary pressure from the local tissue microenvironment, distinct populations of cancer cells – varying in their genetic and epigenetic content – can arise within a tumour (Douglas Hanahan & Weinberg, 2011). Generation of a drug-tolerating subset of cancer cells, usually bearing a point mutation conferring proliferative and anti-apoptotic advantages, could therefore prevent complete tumour regression as resistant cells are selected for and quickly repopulate the tumour following the principles of Darwinian evolution. If critical mutations or signalling pathways responsible for those advantages can be predicted and targeted in advance, the emergence of resistance could be delayed or possibly even prevented, thereby offering a promising approach to improve the eradication of tumours.

1.5.1 Potential mechanisms of resistance to WEE1 inhibitor treatment

The mechanisms underlying the development of resistance to targeted therapies are typically categorised into several classes, including: 1) secondary alterations in the drug target; 2) activation of bypass signalling pathways that drive pro-survival signalling; and 3) alterations in upstream and/or downstream effectors resulting in pathway reactivation (reviewed in Groenendijk & Bernards 2014). Those potential mechanisms of resistance will now be reviewed in relation to the synthetic lethality resulting from loss of SETD2 and WEE1.

1.5.1.1 Secondary alterations in the drug target

The first pathway via which a tumour can develop acquired resistance is through a secondary alteration within the drug target itself. Those alterations, also known as 'gatekeeper' mutations, are responsible for reducing the ability of the small molecule inhibitor to target the kinase. As the WEE1 inhibitor AZD1775 non-covalently interacts with the amino acid residues Ile305, Tyr378 and Cys379 in the ATP-binding domain of WEE1 kinase, mutations occurring in those residues crucial for binding could allow the target molecule to evade inhibition by AZD1775 (Matheson, Venkataraman, et al., 2016).

Another well-studied variation on the secondary alteration leading to acquired resistance is a concept known as 'intragenic suppression'. Intragenic suppression occurs when a phenotype caused by a primary mutation (in this particular situation a loss-of-function mutation in SETD2) is alleviated by a second mutation in the same gene either restoring the original DNA sequence or substituting another amino acid resulting in restoration of protein function closer to wild-type activity (Prelich, 1999). Although gain-of-function mutations in the *SETD2* gene are uncommon (COSMIC database, accessed on 16/07/2017), we might find they could develop under selective pressure.

1.5.1.2 Alterations in upstream and/or downstream effectors resulting in pathway reactivation

In a multi-step pathway, mutations that alter one step of a certain pathway can often be suppressed by a mutation in a second gene that functionally compensates for the defect associated with the primary mutation or inactivation (Prelich, 1999). This second class of suppressors, that can function either up- or downstream of the original mutation or inactivation, is extremely informative as it can help identify other proteins functioning in the pathway of interest.

In this context, Pfister *et al.* have already shown that this synthetic lethality was rescued by expression of either of two mutant forms of RRM2 (T33A and Rxl/Axa), resulting in reactivation of the pathway responsible for the synthesis of ribonucleotides, independent of signalling from upstream steps (Pfister et al., 2015). The mutation in Thr-33 on RRM2 prevents phosphorylation by CDK and ubiquitin-dependent protein degradation is therefore inhibited, resulting in lower sensitivity of SETD2-deficient cells towards the WEE1 inhibitor AZD1775 (D'Angiolella et al., 2012; Pfister et al., 2015). RRM2 mutant Rxl/Axa was found to suppress the synthetic lethality in a similar manner, as Rxl/Axa bears a mutation in residue 49-51 on the CY motif of RRM2, abolishing its interaction with Cyclin F, thus preventing proteolysis of RRM2 (Pfister et al., 2015).

It has also been shown that in the presence of AZD1775, inhibition of either CDK1 by RO3306 or CDK2 by CVT-313 restores RRM2 protein levels and cell viability of SETD2-deficient cells (Pfister et al., 2015). In both cases, the persistent inactivation of CDK1 prevents further signal transduction despite constant inhibition of WEE1 by its inhibitor AZD1775. It can therefore be expected that loss-of-function mutations in either CDK1 or CDK2, both functioning downstream of the targeted kinase WEE1, give rise to resistance to WEE1-inhibitor treatment.

1.5.1.3 Activation of bypass signalling pathways

The third interesting possibility is that the synthetic lethality can be suppressed by an alteration in an alternative pathway. A bypass suppressor might affect the regulation of a pathway that has a related or overlapping function, or the suppressor could alter the activity of a functionally unrelated pathway responsible for maintaining survival and proliferation (Prelich, 1999).

One simple example of this mechanism is when a related but distinct pathway contains a protein B that can substitute for the function of protein A. The redundant protein, Myt1, which also phosphorylates the ATP-binding domain on Tyr-14 and Y15, thereby inhibiting CDK1-cyclin B activity (Booher, Holman, & Fattaey, 1997), could be upregulated in response to treatment with the WEE1 inhibitor AZD1775.

Another example of activation of alternative signalling pathways has already been published, as it was shown that reducing origin firing by depleting replication licensing factors CDC6 or CDT1 suppressed the sensitivity of SETD2-knockout cells toward AZD1775 (Beck et al., 2012; Pfister et al., 2015).

1.6 Aims of this project

The main aim of this project is to identify and elucidate potential resistance mechanisms to WEE1 inhibitor treatment in H3K36me3-deficient cancers. The following describe the stepwise objectives towards this goal:

i. Identify mutants that suppress the synthetic lethality resulting from loss of *set2* and inactivation of *wee1* in *S. pombe* using a genetic screen. Whole genome sequencing of suppressors is used to determine the genomic region and particular mutation that might be responsible for the phenotype.

ii. Select putative suppressors based on function – including those involved in: (1) regulation of G_1/S, intra-S, G_2/M or SAC signalling, (2) regulation of CDK 1/2 activity, (3) regulation of dNTP pools, (4) regulation of transcription initiation or elongation, or (5) regulation of main pathways controlling cell proliferation and survival (RAF1-MEK-ERK1/2 and PI3K-AKT-mTOR) – and extrapolate results from fission yeast to human *SETD2* wild-type and *SETD2* CRISPR knock-out U2OS cell lines.

iii. Validate top hits in renal cancer cell lines 786-O (SETD2 wild-type) and A498 (SETD2 truncating mutation), as well as identify molecular mechanisms by which inactivation of those genes could result in the development of acquired drug resistance to AZD1775.

It is hoped that new insights into the mechanisms of resistance to WEE1 inhibitor treatment in H3K36me3-deficient cancers can contribute to the development of multi-target drug designs, aiming to combat resistance before it emerges.

2 Chapter 2: Methods

2.1 Methods for experiments performed in S. pombe

Yeast strains and media. Strains were cultured and stored as described in Moreno, Klar, & Nurse, 1991. Cells were grown in non-selective, nutrient rich medium (YE6S) at 25 °C for 2-3 days and then stored at room temperature. YE6S medium contained 3% glucose, 0.5% EZmix^{TM} yeast extract (Sigma), and 1.125 g/L supplements mix containing equal amounts of adenine, arginine, L-histidine, L-leucine, lysine, tryptophan, and uracil. Permanent stocks of yeast strains were stored in Nunc cryo-tubes in 0.5 mL YE6S and 0.5 mL YFM at -80°C.

The genotypes of the *S. pombe* strains used in this study are listed in *Table 2.1*.

Table 2.1. List of S. pombe strains used in this study

Strain	***Label***	***Genotype***
TH344*	*wee1-50 h-*	*wee1-50 h-*
TH345*	*wee1-50 h+*	*wee1-50 h+*
TH665	*paf1Δ*	***paf1::G418*** *ade6 - M210. leu1-32, ura4-D18, his3-D1, arg3-D4*
TH2093	*wild type*	*arg3-D4, ade6-D1, ura4-D18, leu1-32, his3-D1 h+*
TH6645	*nse5Δ*	***nse5::G418*** *ade6 - M210. leu1-32, ura4-D18, his3-D1, arg3-D4*
TH6236	*set2Δ*	***set2::kanMX*** *ade6-210 leu1-32 ura4-D18*
TH7121*	*set2Δ wee1-50*	***set2::kanMX*** *wee1-50 ,ade6-D1, ura4-D18, leu1-32, his3-D1*
TH7122*	*set2Δ wee1-50*	***set2::kanMX*** *wee1-50 arg3-D4, ade6-D1, ura4-D18, leu1-32, his3-D1*

*Temperature sensitive strains

Crossing and random spore analysis. Parental *S. pombe* strains (*Table 2.1*) of opposite mating types were mixed in a drop of YE6S medium and grown for 2-3 days at 25 °C on synthetic sporulation agar (SPAS) medium. Conditions of nutrient starvation allowed cells to conjugate and sporulate, resulting in the presence of zygotic asci as visualised by light microscopy (Nikon microscope-Eclipse E400).

For random spore analysis, a 1 µL loop of cells from the desired cross was mixed with 90 µL of Mili-Q water and 10 µL β-glucuronidase, and incubated at 25 °C O/N. Cells were then plated onto YE6S medium with a density of 1 x 10^4 cells/mL and grown for 4-5 days at 25 °C. Desired progeny were identified by replica-plating onto selective media (YE6S and G418 selective medium: 500 µg/ml Geneticin (G418) added post sterilisation).

Liquid cultures and serial dilution assay. Liquid cultures were prepared by inoculating a single colony taken from a fresh agar plate into an appropriate volume of YE6S medium. Cultures were grown O/N with shaking at a temperature of 25 °C. The absorbance at 595 nm (optical density OD_{595}) in a Pharmacia Biotech Ultraspec 2000 was used as a measure of cell density, with an OD_{595} of 0.1 being ~2 x 10^6 cells per ml. Cell cultures were maintained in mid-exponential growth between 2 x 10^6 and 1 x 10^7 cells per ml (OD_{595} between 0.1 to 0.5).

For the serial dilution assay, cell concentration was adjusted to OD_{595} 0.2 in 200 µL, and 5 -fold serial dilutions were subsequently made in YE6S medium. 8 µL of each dilution was then spotted onto appropriate plates. The plates were incubated for 2-3 days at the following temperatures: 25 °C, 32 °C and 35.5 °C, and then photographed using the BIO-RAD Molecular Imager® Gel Doc™ XR+ System with Image Lab.

2.2 Methods for experiments performed in mammalian cells

Cell culture. U2OS (human osteosarcoma) cells were obtained from ATCC (ATCC number HTB-96). The U2OS SETD2 CRISPR knockout cell line was generated by our own group using the CRISPR-Cas9 technology as previously described (Pfister et al., 2015). The target sequence of the chimeric gRNA scaffold was ACTCTGATCGTCGCTACCAT (first exon of *SETD2*) (Pfister et al., 2015).

Human renal cell carcinoma cell lines 786-O (SETD2 wild-type) and A498 (*SETD2* homozygous truncating mutation) were kind gifts from V. Macaulay and E. Hammond, respectively.

U2OS, 786-O and A498 cell lines were cultured in Dulbecco's Modified Eagle's Medium (DMEM) supplemented with 10% v/v foetal bovine serum (FBS, Sigma), penicillin (100 units/mL, Sigma) and streptomycin (0.1 mg/mL, Sigma) at 37°C in a humidified atmosphere containing 5% CO_2

Transient siRNA-mediated gene knockdown. U2OS cells were reverse transfected with short interfering RNAs (siRNAs) (12 nM final concentration) or micro-RNA antisense hairpin inhibitors (20 nM final concentration) using Lipofectamine RNAiMAX (Invitrogen) according to the manufacturer's instructions. Medium was replaced 16-20 hours after transfection.

The target sequences of the siRNAs used in this project are listed below:

ON-TARGETplus Human BUB1 siRNA
siBUB1 #1 (Dharmacon): CGAAGAGUGAUCACGAUUU
siBUB1 #2 (Dharmacon): CAAAGAAGGGUGUGAAACA
siBUB1 #3 (Dharmacon): GAAUGUAAGCGUUCACGAA
siBUB1 #4 (Dharmacon): GCAACAAACCAUGGAACUA

ON-TARGETplus Human CDK1 siRNA
siCDK1 #1 (Dharmacon): GGUUAUAUCUCAUCUUUGA
siCDK1 #2 (Dharmacon): UCGGGAAAUUUCUCUAUUA

siCDK1 #3 (Dharmacon): GUAUAAGGGUAGACACAAA
siCDK1 #4 (Dharmacon): CAAACGAAUUUCUGGCAAA

ON-TARGETplus Human MAP2K1 siRNA
siMAP2K1 #1 (Dharmacon): CCAUGCUGCUGGCGUCUAA
siMAP2K1 #2 (Dharmacon): GAGGUUCUCUGGAUCAAGU
siMAP2K1 #3 (Dharmacon): CGACGGCUCUGCAGUUAAC
siMAP2K1 #4 (Dharmacon): GCACAAGGUCCUACAUGUC

ON-TARGETplus Human PAF1 siRNA
siPAF1 #1 (Dharmacon): CCACUGAGUUCAACCGUUA
siPAF1 #2 (Dharmacon): CUGUAGAAGAGACGUUGAA
siPAF1 #3 (Dharmacon): GAGUACAACUGGAACGUGA
siPAF1 #4 (Dharmacon): GUGCCAUGGAUGCGAAAGA

ON-TARGETplus Human PAK1 siRNA
siPAK1 #1 (Dharmacon): ACCCAAACAUUGUGAAUUA
siPAK1 #2 (Dharmacon): GGAGAAAUUACGAAGCAUA
siPAK1 #3 (Dharmacon): UCAAAUAACGGCCUAGACA
siPAK1 #4 (Dharmacon): CAUCAAAUAUCACUAAGUC

ON-TARGETplus Human PNKP siRNA
siPNKP #1 (Dharmacon): GUGAAACAGCUGGGAGUUA
siPNKP #2 (Dharmacon): CCGGAUAUGUCCACGUGAA
siPNKP #3 (Dharmacon): GACCGGAAGUGCUCCAGAA
siPNKP #4 (Dharmacon): GGAAACGGGUCGCCAUCGA

ON-TARGETplus Human RICTOR siRNA
siRICTOR #1 (Dharmacon): GACACAAGCACUUCGAUUA
siRICTOR #2 (Dharmacon): GAAGAUUUAUUGAGUCCUA
siRICTOR #3 (Dharmacon): GCGAGCUGAUGUAGAAUUA
siRICTOR #4 (Dharmacon): GGGAAUACAACUCCAAAUA

ON-TARGETplus Human CDK1NA siRNA

Non-Targeting (NT) proprietary sequence of supplier (Qiagen)

The target sequences of the microRNA hairpin inhibitor used in this project are listed below:

MiRIDIAN microRNA Human has-miR-106b-5p
Mature microRNA sequence: UAAAGUGCUGACAGUGCAGAU

miRIDIAN microRNA Hairpin Inhibitor Negative Control #1

Drug treatment. All inhibitors were dissolved in Dimethyl sulfoxide (DMSO) and stored at -80 ^{0} C per the manufacturer's instructions. Inhibitors used in this study are listed in *Table 2.2.*

Table 2.2. List of inhibitors and their targets used in this study.

Inhibitor names	*Target*	*Purchased from*
AZD1775 (MK-1775)	WEE1	Axon Medchem

Sample collection and cellular fractionation for Western Blot. Transfected cells were washed with PBS, harvested, and lysed in lysis buffer (50 mM Tris HCl pH 7.5, 150 mM NaCl, 1% Triton) supplemented with 1:50 fresh protease inhibitor cocktail and 1:100 fresh phosphatase inhibitor cocktail (1mM NaOVa; 10mM NaF; 10mM NaPyrophosphate). Lysates were centrifuged for 10 minutes at 17,000 g at 4 °C to pellet cellular debris. The supernatant was subsequently transferred to a fresh Eppendorf tube and protein concentrations were quantified by the Bradford mini-assay using the Pierce Coomassie Plus Assay Reagent.

To isolate cytoplasmic and nuclear fractions, cells were resuspended in 2x buffer A (20 mM HEPES, 20 mM KCl, 680 mM sucrose, 10 mM NEM, 2 mM EDTA and a mixture of protease and phosphatase inhibitors). After addition of 0.1% Triton X-100 (final conc.), the mixture was incubated on ice for 5 minutes. Cells were centrifuged at 5000 g for 10 minutes and the supernatant (cytoplasmic fraction) was frozen at -20 °C. Cell pellets were washed with lysis buffer and nuclei were then incubated in 1 x buffer B (10 mM HEPES, 2 mM NEM, 6 mM EDTA, 0.4 mM EGTA and a mixture of protease and phosphatase inhibitors) for 10 minutes on ice. After 5 min centrifugation at 5000 g, the supernatant (nuclear fraction) was frozen at -20 °C. α-Tubulin was used as a marker of cytoplasm and β-Lamin of nucleus (Mendez *et al.*, 2000).

Western Blotting. Before loading, samples were boiled for 3-5 minutes at 95 °C. Then, 20 µg of protein per lane (using anti- α-Tubulin antibody as loading control) was separated onto a pre-cast NuPAGE Tris-Acetate gel (Invitrogen) followed by transfer onto a polyvinylidene fluoride (PVDF) membrane (0.45 µm pore size) (Invitrogen) according to the manufacturer's

instructions. After transfer, residual binding sites on the membranes were blocked with 4% skimmed milk in PBS-$T_{0.05}$ for 45-60 minutes at room temperature and probed with the appropriate primary antibodies at 4 °C overnight. The membranes were then washed three times with PBS-$T_{0.05}$, followed by incubation with horseradish peroxidase-conjugated (HRP)-conjugated secondary antibodies for 1 hour at room temperature. Antibody reactivity was visualised with the Pierce ECL Western Blotting Substrate (Thermo Scienfitic) using the ChemiDoc^{TM} MP Imaging System (BioRad) as per the manufacturer's instructions. The relevant bands were scanned and quantified using ImageLab Software 5.2.1. After this, the blot was either stripped and re-probed, or washed in PBS, wrapped in cling film and stored at 4ºC.

Targets of the primary antibodies used for western blotting are as follows: Apoptosis Cocktail (pro/p17-caspase-3, cleaved caspase-3, cleaved-PARP, cleaved-actin, 1:500, Abcam), Bub1 (1:1000, Abcam), p21 Waf1/Cip1 (1:1000, Cell Signaling), MEK1 (1:2000, Cell Signaling), Oct4 (1:1000, Abcam), PAF1 (1:1000, Abcam), PAF1* (Cell Signaling, 1:1000), PAF1 (1:1000, ThermoFisher Scientific), PAK1 (Cell Signaling, 1:1000), PNK (1:1000, Abcam), R2 N-18 (1:2000, Santa Cruz), Rictor (1:1000, Cell Signaling). Secondary Alexa Fluor antibodies were purchased from Invitrogen.

*This antibody was used for most experiments

Quantitative RT-PCR (Reverse Transcription-Polymerase Chain Reaction). Total RNA was purified from cell pellets with the RNeasy mini kit (Qiagen). RNA concentration was determined using a Nanodrop 1000 spectrophotometer (Thermo Scientific). Purified total RNA (1 µg) was reverse transcribed using the superscript iii first strand synthesis supermix for qRT PCR kit (Invitrogen), according to the manufacturer's instructions. Quantitative RT-PCR was performed using Absolute Blue QPCR SYBR green, low ROX Mix (Thermo

Scientific). Reactions were carried out in duplicate for each target transcript using a 7500 Fast Real-Time PCR System (Applied Biosystems).

The comparative CT method was applied for quantification of gene expression, and values were normalized against GAPDH as control. Results were expressed as fold change in mRNA levels. The following primers, as described in Zhang *et al.* (2011) were used:

hOCT4 Forward	TTCAGCCAAACGACCATCTG
hOCT4 Reverse	CACGAGGGTTTCTGCTTTGC

Resazurin assay for cell viability. 72 hours after cells were challenged with AZD1775, culture medium was removed and fresh medium containing 10 µg/mL resazurin was added to each well. The fluorescent signal is proportional to the number of living cells, and was measured by a fluorescence plate reader (BMG Labtech POLARstar OMEGA) after 2 hours of incubation at 37 °C.

Statistical analysis. Unless stated otherwise, all data in the figures and corresponding text are expressed as the mean +/- SEM of n samples ($n \geq 3$). Student's unpaired t-tests were used for comparisons between two or more experimental groups, without assuming a consistent SD. P-values of <0.05 were considered statistically significant.

3 Chapter 3: Results

3.1 Initial suppressor screen in fission yeast

In order to explore the possible mechanisms of resistance to WEE1 inhibitor treatment in H3K36me3-deficient cells – a synthetic lethal interaction previously described in *Chapter 1.4* – an initial screen was performed in fission yeast (*S. pombe*) by other members in my lab (see *acknowledgements*). The main aim was to identify spontaneous mutants that suppressed the *set2Δ wee1-50* temperature sensitivity.

The suppressor screen was set up as follows: a population of *set2Δ wee1-50* cells was plated onto YE6S plates at high density (1×10^4 to 1×10^6 cells per mL) and incubated for 4-5 days at the restrictive temperature of 35.5 °C (*Figure 3.1a*). Colonies that grew at the restrictive temperature were picked and purified by repeated streak-plating.

In total, a number of 23 spontaneous suppressors of the *set2Δ wee1-50* lethality were isolated (named ss3-ss25). Whole genome sequencing of these suppressor strains was performed in order to determine the genomic region and particular mutation that was responsible for the phenotype. Many suppressor mutants carried overlapping genomic fragments and in total were found to represent 83 genomic regions. This gene set was enriched for genes involved in cellular and metabolic processes, including cell cycle regulation, chromosome separation, and biosynthesis as revealed by analysis of Gene Ontology (GO) biological process term enrichment (*Figure 3.1b*).

The putative suppressors were divided into three main classes of interest, including (i) genes functioning as cell cycle regulators, (ii) genes involved in cell communication pathways and (iii) genes involved in transcription (*Figure 3.1c*).

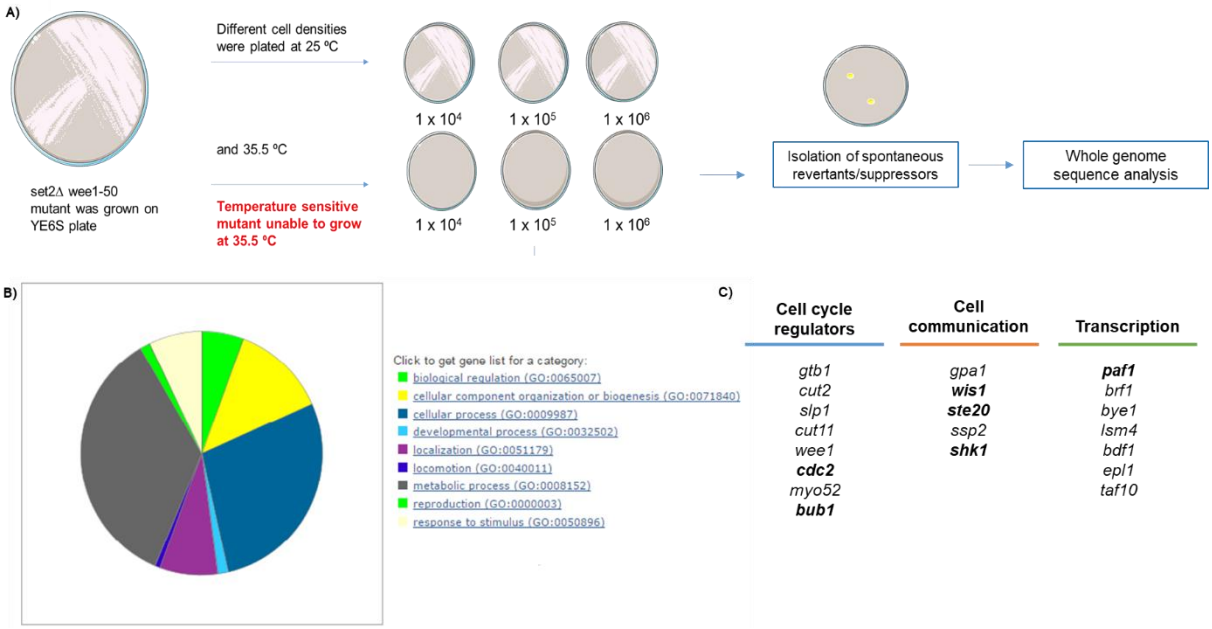

Figure 3.1. Initial suppressor screen of the set2Δ wee1-50 synthetic lethality results in the identification of 83 candidate suppressors in S. pombe. A) *Experimental design of the suppressor screen. Putative suppressor genes were identified by whole genome sequencing.* ***B)*** *The pie chart slices represent the percent of putative suppressors identified in a particular category as revealed by gene ontology term enrichment analysis.* ***C)*** *Summary of mutations present in 23 isolated mutant strains (ss3-ss25), showing three different classes of mutants in cell cycle regulation, cell communication, and transcription. Genes shown in bold were selected for further studies in mammalian cell lines.*

As described above, class (i) suppressors included a number of genes involved in cell cycle regulation. Among the mutations identified here was one putative revertant, i.e. a secondary substitution in the *wee1* gene that was predicted to restore the function of this protein, in addition to two mutations in a neighbouring non-coding RNA, predicted to increase the expression of Wee1 (*Figure 3.1c*). Furthermore, four potential extragenic suppressors in the downstream effector kinase Cdc2/Cdk1 were identified (*Figure 3.1c*). Three out of four mutations in *cdc2* introduced a premature stop codon and the fourth mutation caused an alteration resulting in the replacement of the codon specifying Thr-14 (T14A) in Cdc2 with the non-phosphorylatable residue asparagine. Several other putative secondary suppressor mutations were detected, including one insertion in the *bub1* gene, which has an important role in SAC signalling, and one substitution in *cut2*, required for the onset of anaphase in fission yeast (Jia, Li, & Yu, 2016; Yanagida, 2000).

Class (ii) suppressors were described as genes involved in cell communication and this class was particularly enriched for components and/or regulators of the MAPK signalling pathway. Putative suppressors in class (ii) included MAP kinase kinase *wis1*, serine/threonine kinase *ste20* and the p21-activated kinase *shk1* (*Figure 3.1c*).

Class (iii) suppressors included a number of factors associated with the transcription machinery in fission yeast. Mutations in the genomic region encoding RNA-polymerase II associated factor *paf1* were observed in 10 out of 23 *S. pombe* suppressor strains (*Figure 3.1c*). Furthermore, TATA-box binding protein associated factor 10 (*taf10*) was found to be mutated in six of the suppressor strains (*Figure 3.1c*).

A large number of the genes putatively responsible for suppression of the *set2Δ wee1-50* temperature sensitivity in *S. pombe* have human orthologs and the initial screen data could therefore provide an excellent starting point for the identification of mechanisms of resistance to WEE1 inhibitor treatment in H3K36me3-deficient human cancer cells.

Therefore, genes involved in either of the following pathways/processes, including (1) regulation of CDK1/2 activity, (2) regulation of G_1/S, intra-S, G_2/M or SAC signalling, (3) regulation of dNTP pools, (4) regulation of transcription initiation or elongation, or (5) regulation of main pathways controlling cell proliferation and survival (RAF1-MEK-ERK1/2 and PI3K-AKT-mTOR), were selected and further studied in mammalian cell lines (*Figure 3.1c*, in **bold**). The major aim of the follow-up experiments was to further characterise the role of the six selected human orthologs, including *BUB1*, *MEK1/MAP2K1*, *PAF1*, *PAK1*, *PNKP* and *RICTOR*, in mediating suppression of the synthetic lethality resulting from loss of SETD2 and WEE1.

3.2 Validation of AZD1775-sensitivity in *SETD2* WT and *SETD2* CRISPR KO U2OS cells

Prior to validation of the putative synthetic lethality suppressors in mammalian cells, WEE1 inhibitor sensitivity was studied in both H3K36me3-proficient and -deficient U2OS osteosarcoma cell lines.

In order to do so, *SETD2* wild-type (WT) and *SETD2* CRISPR knockout (KO) U2OS cells were treated with different concentrations of the WEE1 inhibitor AZD1775. As previously described (Pfister et al., 2015), CRISPR/Cas9 technology was used to introduce a frameshift mutation and a premature stop codon in both *SETD2* alleles, resulting in loss of the SETD2 protein in *SETD2* KO U2OS cells. The *SETD2* KO U2OS cells were found to be hypersensitive to AZD1775 when compared to the *SETD2* WT U2OS cells (KO IC_{50} (half maximal inhibitory concentration) = 187 nM versus WT IC_{50} = 562 nM) (*Figure 3.2*).

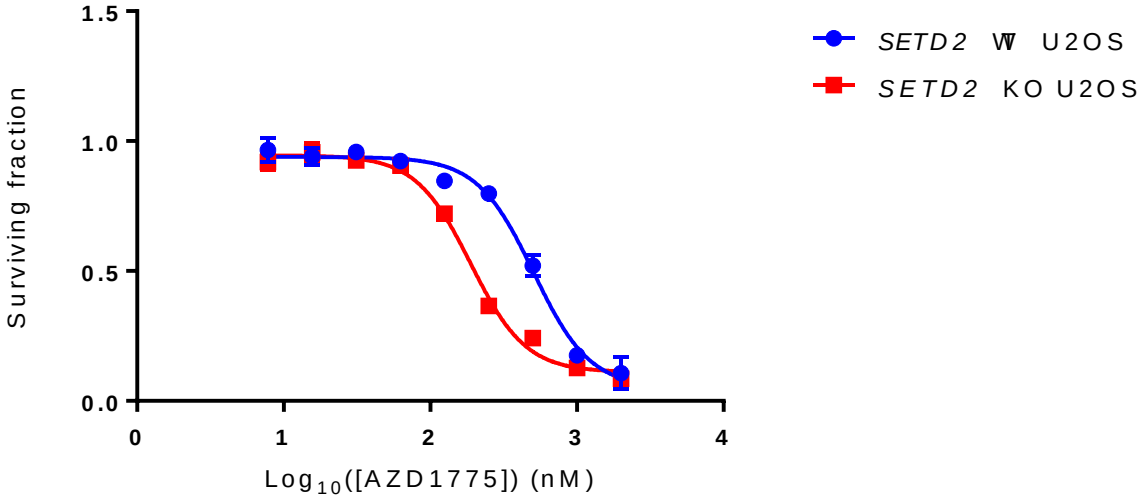

Figure 3.2. WEE1 inhibition selectively kills H3K36me3-deficient cancer cells. *Non-linear regression four-parameter dose-response curves for the cell viability of SETD2 WT and SETD2 CRISPR KO U2OS cells following 72 h exposure to 7.813, 15.63, 31.25, 62.50, 125.0, 250.0, 500, 1000 and 2000 nM concentrations of the WEE1 inhibitor AZD1775.*

3.3 Verification of knockdown efficiency in *SETD2* WT and *SETD2* CRISPR KO U2OS cells

In order to assess the effect of down-regulating BUB1, MEK1, PAF1, PAK1, PNKP, and RICTOR on AZD1775-response in both *SETD2* WT and *SETD2* KO U2OS cells, siRNA-mediated gene silencing was used to specifically inhibit those genes.

Non-targeting control pools as well as four individual siRNAs (siRNAs #1 through #4), each containing an individually defined siRNA sequence against each target gene (*BUB1, MEK1, PAF1, PAK1, PNKP* and *RICTOR*) (see *Chapter 2.2),* were transfected into U2OS cells at a final concentration of 12 nM.

Transfection of both *SETD2* WT and *SETD2* CRISPR KO cells with siRNA pools #1-4 against BUB1, PAF1 and PNKP resulted in a substantial decrease in protein levels from 48 to 96 hours post-transfection as judged by Western Blotting (*Figure 3.3 b, c and d*). Mock transfection with a non-targeting siRNA control failed to reduce target-protein expression in both *SETD2* WT as well as *SETD2* CRISPR KO U2OS cells.

The siRNA pools #1-4 against RICTOR, MEK1 and PNKP did not all show similar on-target activity and only those effectively reducing target-protein expression – being siRICTOR pool #2, siMEK1 pool #1, siMEK1 pool #2 and siPAK1 pool #1 – were selected for further experiments (*Figure 3.3 a, e and f*).

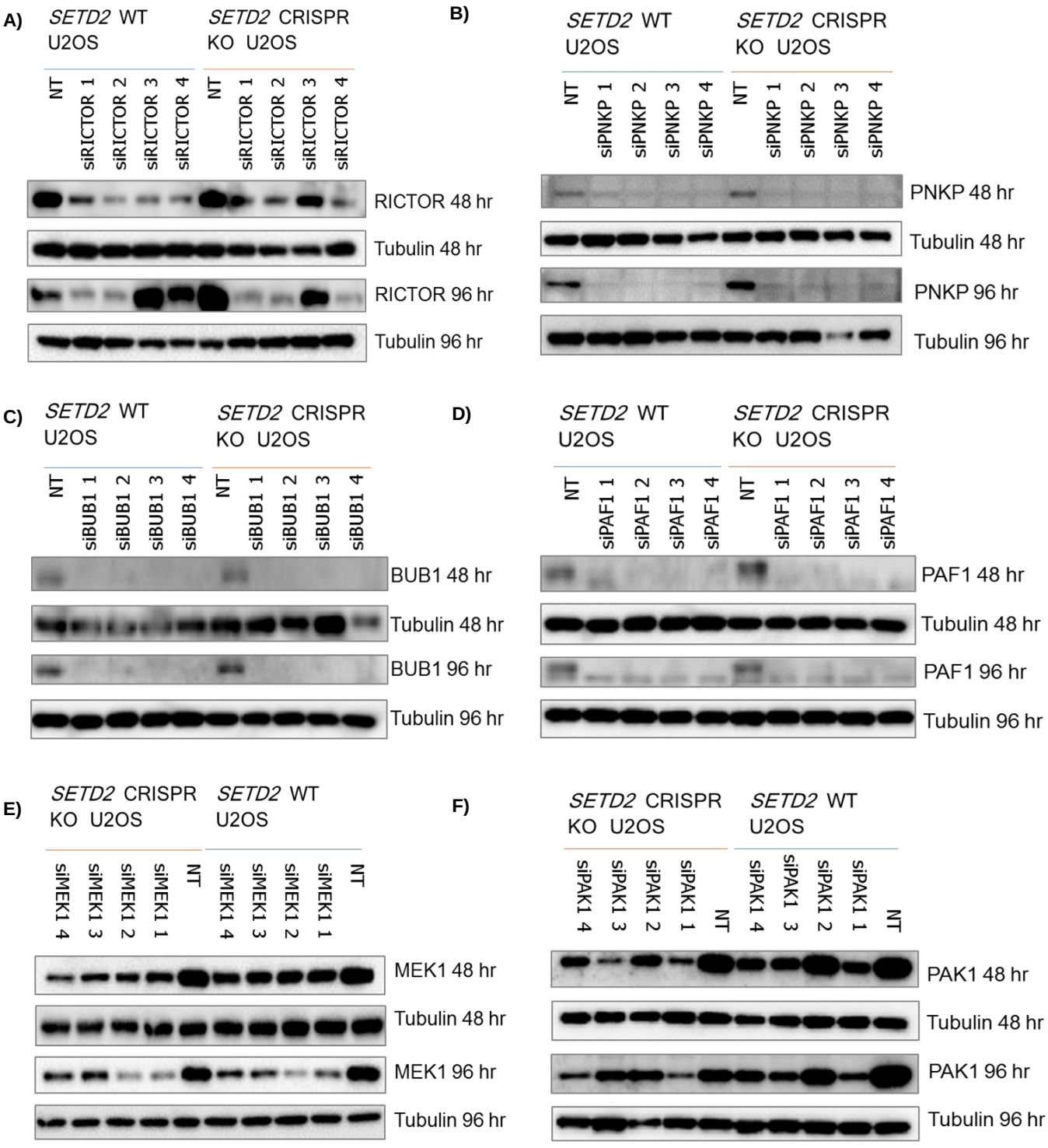

Figure 3.3. Overview Western Blots to confirm silencing efficiency. *SETD2 WT and SETD2 CRISPR KO U2OS cells were transfected with 12 nM concentrations of specific siRNAs (#1 through #4) directed against RICTOR (200 kDa)* ***(A)****, PNKP (57 kDa)* ***(B)****, BUB1 (122 kDa)* ***(C)****, PAF1 (80 kDa)* ***(D)****, MEK1 (45 kDa)* ***(E),*** *and PAK1 (68 kDa)* ***(F)****. Tubulin was used as a loading control.*

3.4 Effect of BUB1, MEK1, PAF1, PAK1, PNKP and RICTOR knockdown on cell viability in U2OS cells in the presence of AZD1775

After siRNA silencing efficiency was validated for all six candidate genes (see *Chapter 3.3*), *SETD2* WT and *SETD2* CRISPR KO U2OS cells were transfected with BUB1, MEK1, PAF1, PAK1, PNKP, or RICTOR siRNA. 72 hours post-transfection, cells were treated with either DMSO (600 nM) or the WEE1 inhibitor (75, 150, 300, or 600 nM) and subjected to a resazurin reduction assay to determine cell viability 48 hours after AZD1775-treatment.

Knockdown of the human cyclin-dependent kinase 1 (hCDK1) was used as a positive control, as four putative loss-of-function mutations in yeast homologue cell division cycle 2 (*cdc2*) were found to suppress the synthetic lethality between *set2Δ* and *wee1-50* (*Figure 3.1c*). As demonstrated in *Figure 3.4a*, knockdown of hCDK1 did significantly restore cell viability of both *SETD2* WT and *SETD2* CRISPR KO U2OS cells in the presence of AZD1775.

Viability of *SETD2* WT and *SETD2* CRISPR KO cells was, however, not significantly affected by MAP2K1, PAK1, PNKP or RICTOR siRNA-interference treatment (*Figure 3.4 b, c and d,* and *Figure 3.5c*).Knockdown of PAF1 partially rescued cell viability by higher concentrations of the WEE1 inhibitor AZD1775 (300 and 600 nM) in *SETD2* WT and *SETD2* CRISPR KO U2OS cells (*Figure 3.5b*). The I_{max}% values (representing the survival rate at maximum inhibition), differed significantly between non-targeting control siRNA and PAF1 siRNA treated U2OS cells, with a stronger effect observed in the *SETD2* CRISPR KO U2OS cells (non-targeting siRNA control I_{max}% = 9.703e-003 versus PAF1 siRNA I_{max}% 41.56, p*= 0.0294). Furthermore, cell viability studies revealed that knockdown of SAC kinase BUB1 significantly reduced sensitivity of *SETD2* CRISPR KO cells to 300 and 600 nM of AZD1775 (*Figure 3.5d*)

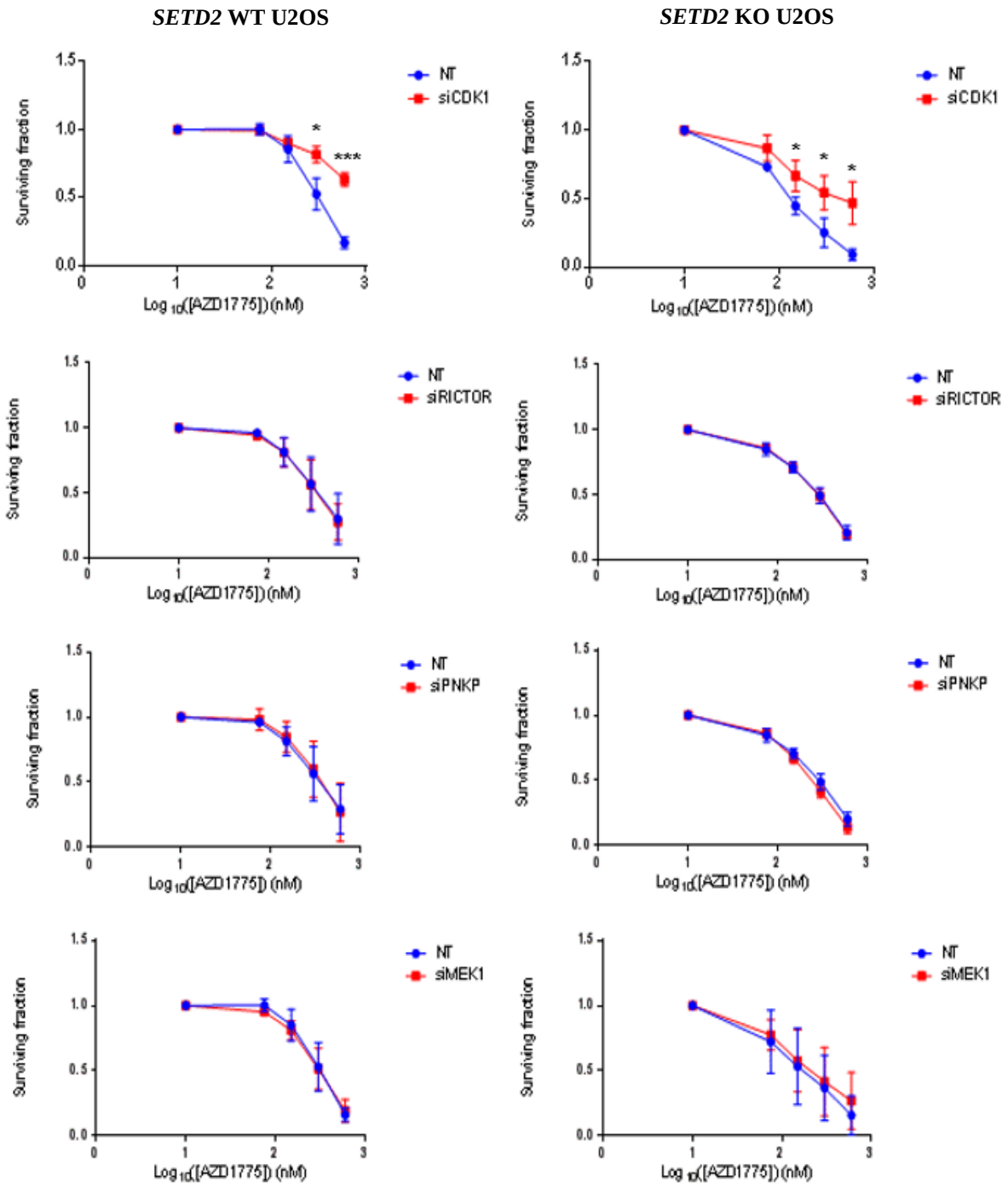

Figure 3.4. Survival fraction of CDK1 (A), RICTOR (B), PNKP (C) or MEK1 (D) siRNA treated SETD2 WT and SETD2 CRISPR KO U2OS cells *after 72 h exposure to different concentrations of AZD1775 (75, 150, 300 and 600 nM). Data points and bars represent the mean and standard error of at least three independent experiments.*

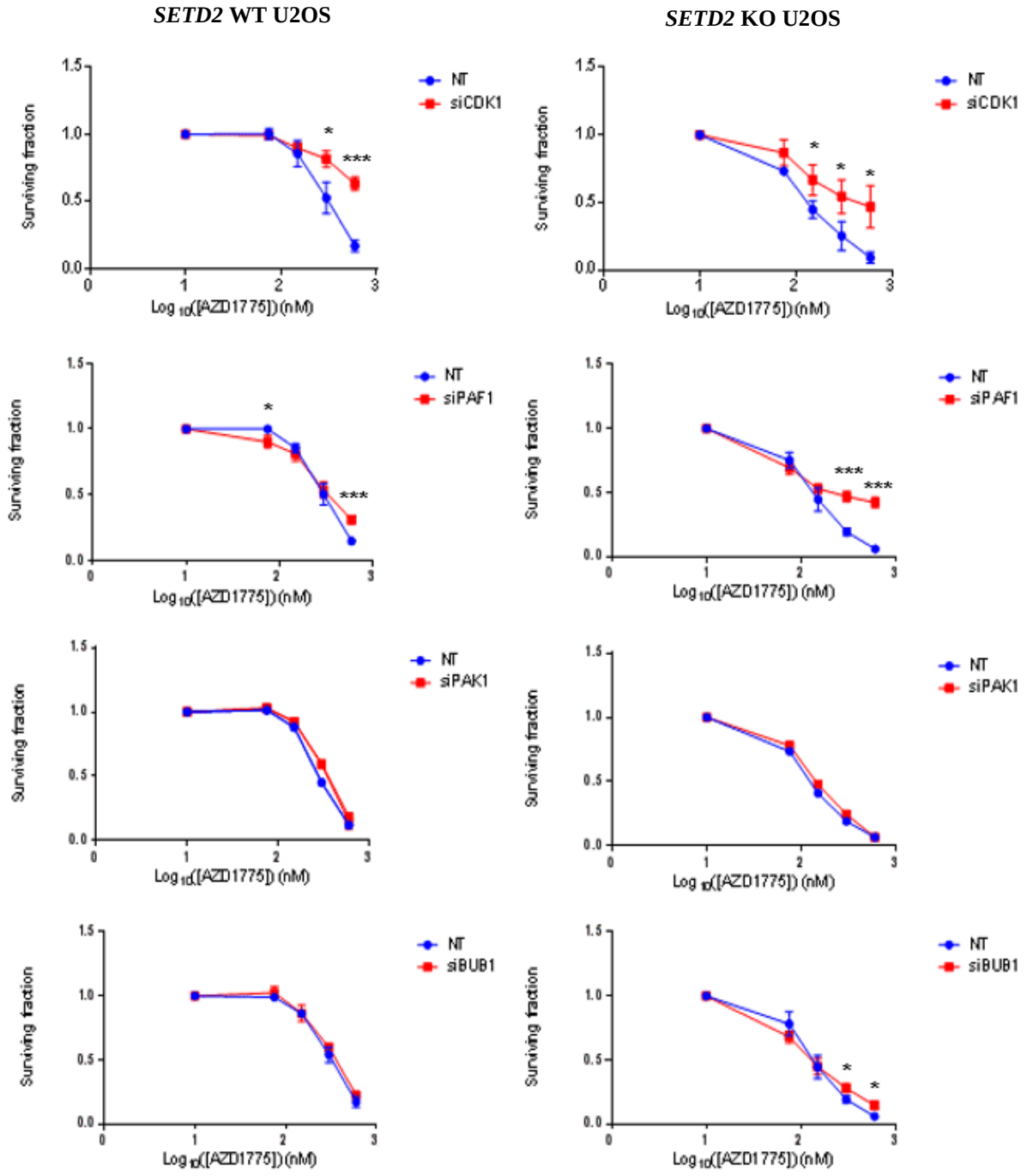

Figure 3.5. Survival fraction of CDK1 (A), PAF1 (B), PAK1 (C) or BUB1 (D) siRNA treated SETD2 WT and SETD2 CRISPR KO U2OS cells *after 72 h exposure to different concentrations of AZD1775 (75, 150, 300 and 600 nM). Data points and bars represent the mean and standard error of at least three independent experiments.*

3.5 Effect of PAF1 knockdown on cell viability in renal cancer cell lines 786-O and A498 in the presence of AZD1775

As knockdown of PAF1 had the strongest effect on WEE1-inhibitor sensitivity (*Figure 3.5)*, and its phenotype strongly resembled that observed following knockdown of hCDK1, subsequent experiments were conducted to validate this suppressor phenotype in different systems, as well as elucidate the mechanisms by which PAF1 modulates response to AZD1775.

In order to investigate whether knockdown of PAF1 also affects cell viability in response to WEE1 inhibitor treatment in other cell types, ccRCC cell lines 786-O and A498 were subjected to a resazurin assay as previously described. 786-O expresses wild-type SETD2, but A498 expresses a non-functional SETD2 protein, rendering it hypersensitive to AZD1775 (A498 IC_{50} = 99 nM versus 786-O IC_{50} = 156.7) (*Figure 3.6c*).

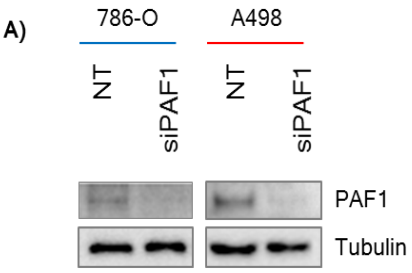

C)

	786-O	786-O	A498	A498
siPAF1	-	+	-	+
IC50	156.7	83.25	99.09	61.14
Imax%	25.65	44.47	20.45	38.74

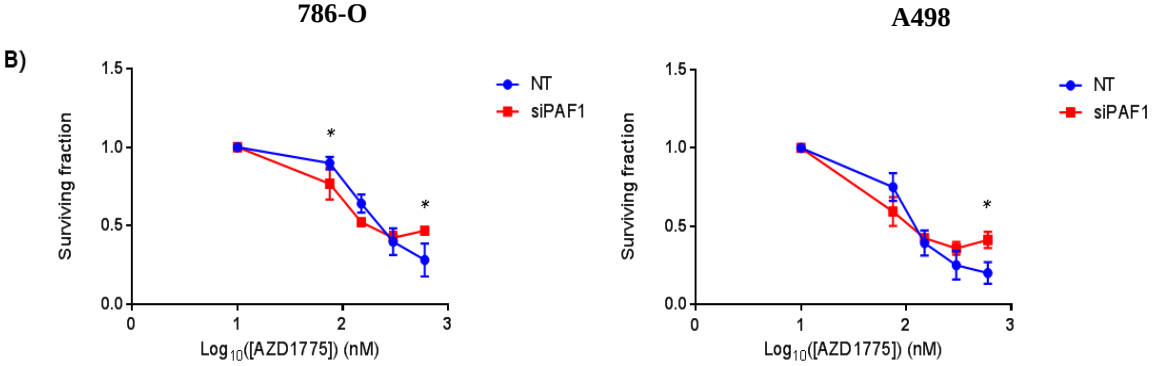

Figure 3.6. Effect of PAF1 silencing on cell viability in the presence of AZD1775. A) *siRNA silencing efficiency validation for PAF1 by Western Blot in both 786-O and A498 cells.* ***B)*** *Survival fraction of PAF1 siRNA treated 786-O and A498 cells after 72 h exposure to different concentrations of AZD1775 (75, 150, 300 and 600 nM). Data points and bars represent the mean and standard error of three independent experiments.* ***C)*** *$I_{max\%}$ and IC_{50} (nM) values for both the non-targeting control siRNA and PAF1 siRNA treated renal cancer cells were estimated based on fitting four-parameter logistic dose response equation.*

Knockdown of PAF1 significantly desensitized 786-O and A498 cells to the highest concentration (600 nM) of AZD1775 (*Figure 3.6b*). Western blot analysis was used to verify knockdown efficiency of PAF1 expression (*Figure 3.6a*).

I_{max}% and IC_{50} values for both non-targeting control siRNA and PAF1 siRNA treated RCC cell lines were estimated based on fitting four-parameter logistic dose response equation (*Figure 3.6c).* I_{max}%-values almost doubled upon knockdown of PAF1 in both 786-O and A498 cells, indicating higher survival rates at maximal WEE1-inhibition (*Figure 3.6c*).

3.6 Role of *paf1*Δ in suppression of *set2*Δ *wee1-50* lethality in fission yeast

Although mutations in the genomic region encoding components of the Paf1c and Nse5, the latter a component of the Smc5-Smc6 holocomplex, were observed in 10 out of 23 suppressor strains, the relative contributions of these two genes (*paf1* vs. *nse5*) to suppression of *set2*Δ *wee1-50* lethality in fission yeast still remained unclear.

Therefore, both *set2*Δ *wee1-50 paf1*Δ and *set2*Δ *wee1-50 nse5*Δ triple mutant strains were generated to determine whether either or both suppressed the synthetic lethality of the *set2*Δ*wee1-50* strain using a serial dilution assay. At the permissive temperature of 35.5 °C, growth of the *set2*Δ *wee1-50* double mutant was completely compromised (*Figure 3.7a and b*) as previously found (our unpublished results).

The temperature sensitive phenotype of the *set2*Δ *wee1-50* double mutant was found to be slightly suppressed following deletion of *nse5*, as indicated by growth at the restrictive temperature of 35.5 °C (*Figure 3.7b*).

Deletion of *paf1*, however, suppressed the *set2*Δ *wee1-50* synthetic lethality more efficiently, as the *set2*Δ *wee1-50 paf1*Δ triple mutants appeared to grow even better than the *set2*Δ *wee1-50 nse5*Δ triple mutants (*Figure 3.7a and b*). Those results suggest that Paf1-mediated suppression of Wee1 inactivation is conserved from fission yeast to human cells.

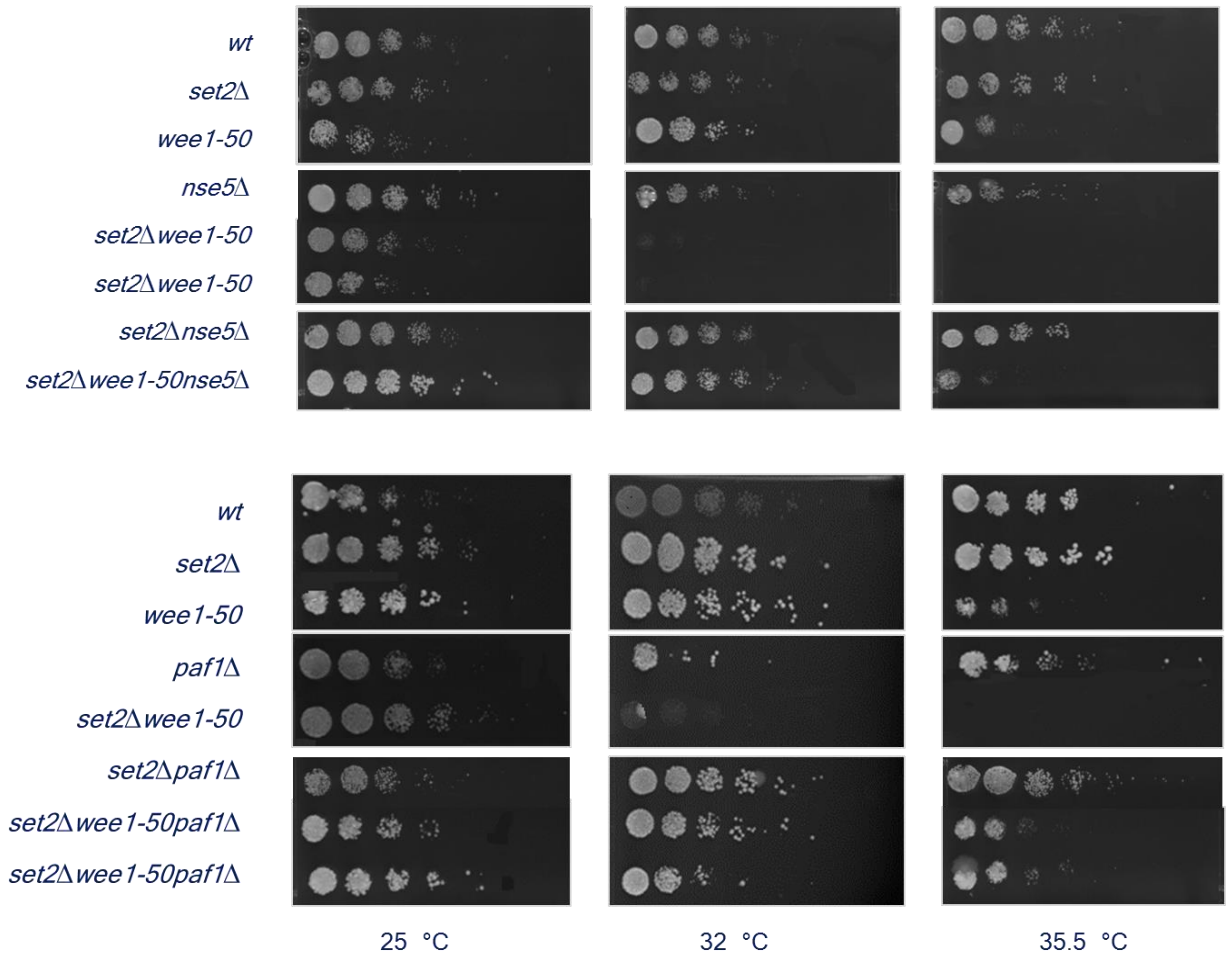

Figure 3.7. Response of set2*Δ *paf1*Δ *and set*Δ *nse5*Δ *double mutants to Wee1 inactivation. *The growth response of wild-type, set2*Δ*, wee1-50, paf1*Δ*, nse*Δ*5, set2*Δ *wee1-50, set2*Δ *paf1*Δ*, set*Δ *nse5*Δ*, set2*Δ *wee1-50 paf1*Δ *and set2*Δ *wee1-50 nse5*Δ *was compared by spotting 5-fold serial dilutions of each strain onto YE6S medium. Plates were the incubated for an appropriate time at either 25, 32 or 35.5 °C.*

3.7 Evaluation of caspase 3-mediated apoptosis in siPAF1 treated U2OS cells in the presence of AZD1775

In order to determine whether the decreased sensitivity to AZD1775 observed in siPAF1 treated U2OS cells was due to reduced levels of apoptosis, caspase 3-activation and corresponding PARP1-cleavage were determined using Western Blot.

In accordance with previous findings by Pfister *et al.* (2015), the apoptotic rate was induced in *SETD2* WT and *SETD2* KO U2OS cells treated with 200 nM AZD1775 when compared to the DMSO-treated control cells, as indicated by elevated levels of cleaved caspase-3 and PARP (*Figure 3.8a*). Furthermore, the increase in levels of cleaved caspase-3, a key executor of the apoptotic process, was stronger in *SETD2* KO U2OS cells than in *SETD2* WT U2OS cells, consistent with increased sensitivity of *SETD2* KO U2OS to WEE1 inhibition (*Figure 3.2 and 3.8b*).

In *SETD2* KO U2OS cells, however, the increase in cleaved caspase 3 levels owing to AZD1775 treatment (200 nM) was several-fold lower in PAF1 siRNA treated U2OS cells than in cells treated with a non-targeting siRNA control, indicative of lower apoptotic rates in PAF1 siRNA treated *SETD2* KO U2OS cells in response to WEE1 inhibitor treatment (*Figure 3.8a* and *3.8b*)

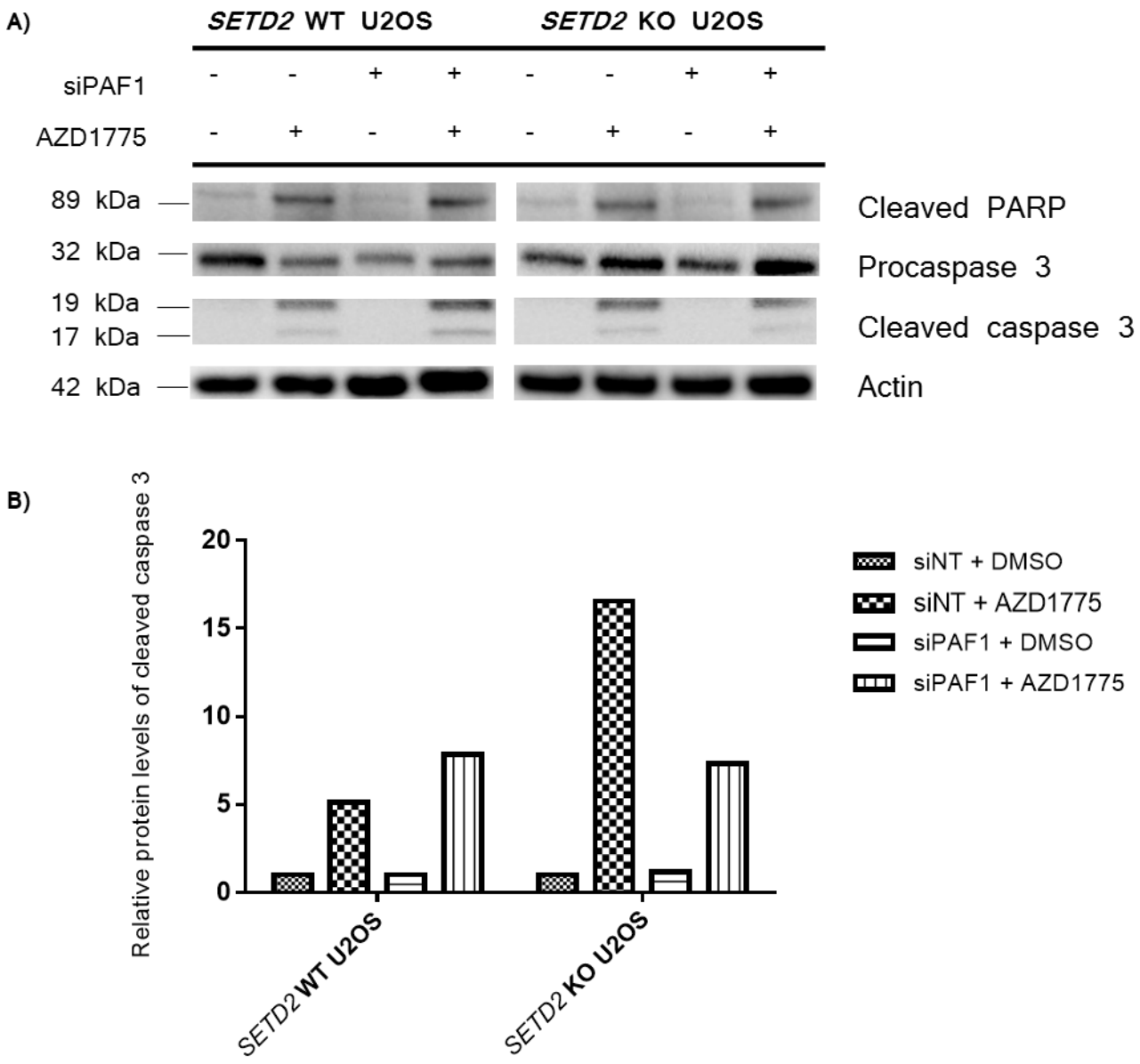

Figure 3.8. Apoptotic response of PAF1 siRNA vs. control siRNA treated U2OS cells in the presence of AZD1775. A) *Cleaved PARP, procaspase 3, cleaved caspase 3 and actin protein expression in SETD2 WT and SETD2 CRISPR KO U2OS cells following treatment with either 200 nM DMSO or 200 nM AZD1775 was assessed using Western Blot.* ***B)*** *Quantitative analysis of cleaved caspase-3 protein levels in control siRNA vs. siPAF1 siRNA treated SETD2 WT and SETD2 CRISPR KO U2OS cells following incubation with AZD1775 for 24 hours.*

In *SETD2* WT U2OS cells, on the other hand, PAF1 siRNA treatment did not appear to have an effect on the apoptotic rate in response to treatment with 200 nM of AZD1775, which is consistent with similar survival fractions of non-targeting control siRNA vs PAF1 siRNA treated *SETD2* WT U2OS cells at this concentration (*Figure 3.5, 3.8a and b*).

3.8 Detection of p21$^{Cip1/Waf1}$ protein levels in *SETD2* WT and *SETD2* CRISPR KO U2OS cells

Next, the possible mechanisms by which loss of PAF1 modulates caspase-3 activity in response to WEE1 inhibitor treatment, were investigated. Several studies have demonstrated that p21$^{Cip1/Waf1}$ inhibits apoptosis by interacting with procaspase 3 to block the activation of caspase-3 (A. Suzuki, Tsutomi, Akahane, Araki, & Miura, 1998; a Suzuki, Tsutomi, Miura, & Akahane, 1999). Furthermore, p21$^{cip1/waf1}$ is a well-characterised CKI, capable of inhibiting all cyclin/CDK complexes (Sherr & Roberts, 1995). Therefore, it was hypothesized that AZD1775-resistance following PAF1 knockdown was due, at least in part, to increased levels of the anti-apoptotic protein p21$^{Cip1/Waf1}$.

To test this hypothesis, p21$^{Cip1/Waf1}$ protein levels were analysed following PAF1 knockdown in both *SETD2* WT and *SETD2* KO U2OS cells. Western Blotting revealed a substantial difference in total p21$^{Cip1/Waf1}$ protein levels between PAF1-treated U2OS cells and the controls (*Figure 3.9a*). Individual band densities were quantified and the ratios of p21$^{Cip1/Waf1}$ protein levels in PAF1 siRNA vs. control siRNA treated U2OS cells were calculated. The ratio was approximately 1.8 in *SETD2* WT U2OS cells and 1.3 in *SETD2* CRISPR KO cell lines, suggesting that p21$^{Cip1/Waf1}$ protein levels are upregulated following knockdown of PAF1.

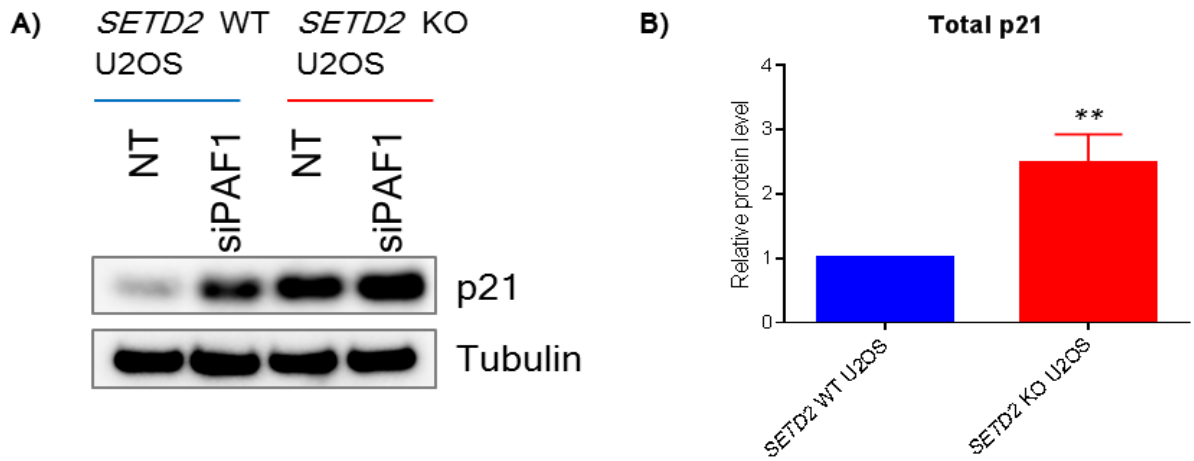

Figure 3.9. Up-regulation of p21$^{Cip1/Waf1}$ in response to loss of SETD2. ***A)*** *Western blot analysis of p21$^{Cip1/Waf1}$ protein levels in SETD2 WT and SETD2 CRISPR KO cells exposed to either non-targeting control siRNA or PAF1 siRNA. A representative example of 3 independent experiment is shown.* ***B)*** *Quantitative analysis of total p21$^{Cip1/Waf1}$ protein levels in control siRNA treated SETD2 WT and SETD2 CRISPR KO U2OS cells. The graphs represent the results of three independent experiments. (P** = 0.0045).*

Interestingly, Western Blot analysis also revealed that basal protein levels of p21$^{Cip1/Waf1}$ were higher in *SETD2* KO U2OS cells when compared to *SETD2* WT U2OS cells (*Figure 3.9a*). Quantitative analysis showed a significant (P-value** = 0.0045) 2-to-3-fold increase in p21$^{Cip1/Waf1}$ protein levels upon loss of *SETD2* in U2OS cells (*Figure 3.9a and b*). Very similar observations have recently been made in SETD2 CRISPR KO skeletal muscle myoblast cells (Yi et al., 2017).

As p21$^{Cip1/Waf1}$ protein function is also affected by its subcellular localisation, I investigated whether the increase of total levels of p21$^{Cip1/Waf1}$ resulted from an increase in either nuclear levels, cytosolic levels, or both. In order to do this, subcellular fractionation was performed and levels of p21$^{Cip1/Waf1}$ were subsequently determined in both fractions using Western Blot (see C*hapter 2.2*). Immunoblotting for Lamin B and α-Tubulin validated the quality of the nuclear and cytoplasmic fractions, respectively. The ImageLab program was used to quantify the amount of p21$^{cip1/waf1}$ signals (*Figure 3.10b*).

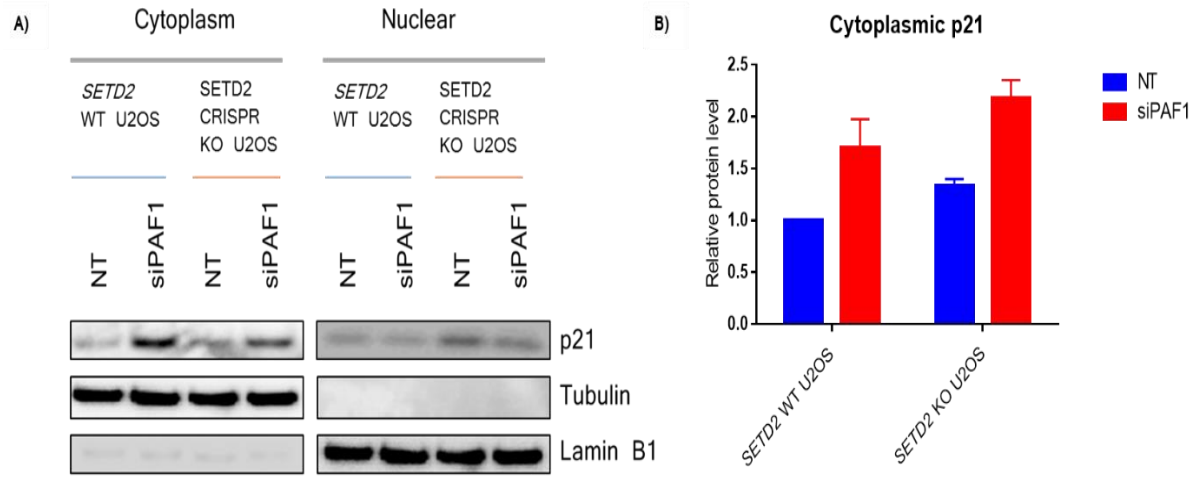

Figure 3.10. Nuclear and cytosolic levels of p21$^{Cip1/Waf1}$ in PAF1 siRNA vs. control siRNA treated U2OS cells. A) *The subcellular localization of p21 in non-targeting control vs. PAF1 siRNA treated U2OS cells was investigated with Western Blot analysis using fractionated protein samples. Lamin B1 was used as a nuclear control, whereas α-Tubulin was used as a loading control.* ***B)*** *Quantitative analysis of cytoplasmic p21$^{Cip1/Waf1}$ protein levels in control siRNA treated SETD2 WT and SETD2 CRISPR KO U2OS cells (n = 2).*

As shown in *Figure 3.10a*, levels of both nuclear and cytoplasmic p21$^{Cip1/Waf1}$ were found to be higher in non-targeting control siRNA treated *SETD2* KO cells than in WT U2OS cells, in accordance with the upregulation of total levels of p21 in *SETD2* KO U2OS cells as shown in *Figure 3.9a and b*.

Furthermore, following siRNA-mediated knockdown of PAF1, there was a strong increase in cytoplasmic levels of p21 in both *SETD2* WT and *SETD2* KO U2OS cells, whereas nuclear p21$^{Cip1/Waf1}$ levels remained relatively unchanged (*Figure 3.10a*). Quantification revealed cytoplasmic levels of p21$^{Cip1/Waf1}$ were around 1.7-fold higher in PAF1 siRNA than in control siRNA treated U2OS cells, independent of *SETD2* mutational status (*Figure 3.10b*). These findings suggest that PAF1 may have an additional role in regulating intracellular distribution of p21$^{Cip1/Waf1}$.

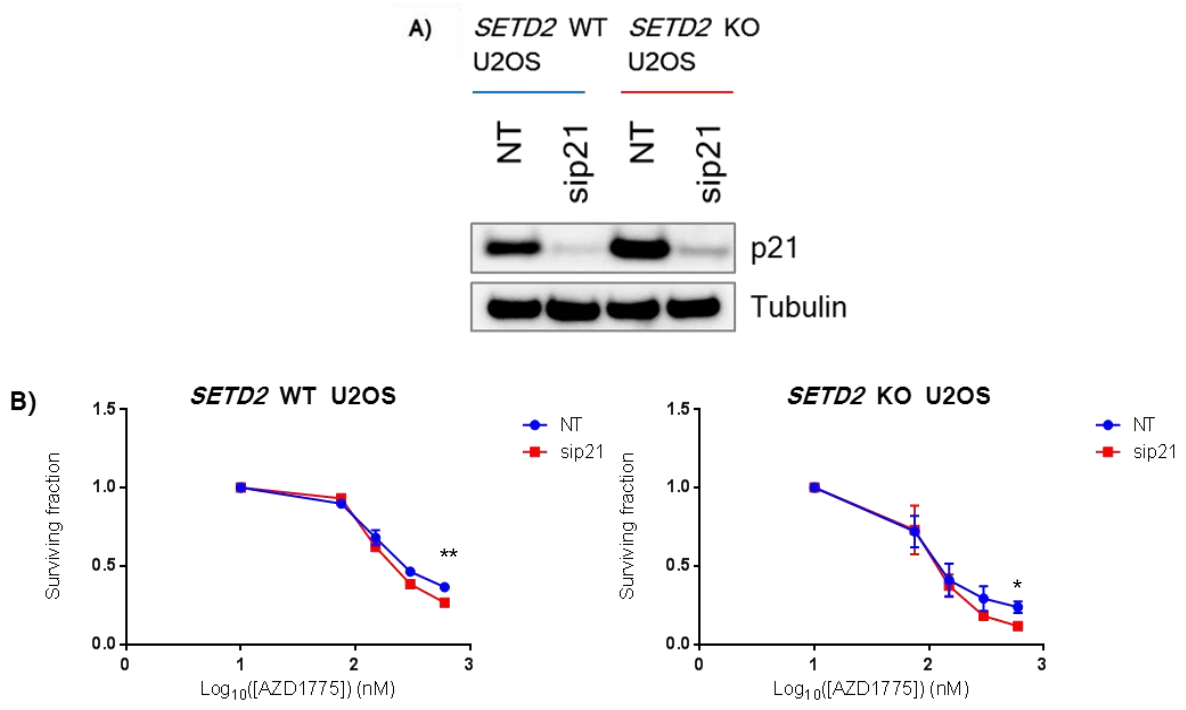

Figure 3.11. Role of p21 in mediating AZD1775-induced cell death. A) *siRNA knockdown efficiency validation for p21 by Western Blot in both SETD2 WT and SETD2 CRISPR KO U2OS cells.* ***B)*** *Downregulation of p21 in AZD1775-sensitive SETD2 WT and SETD2 CRISPR KO U2OS cells leads to a small decrease in cell viability upon WEE1 inhibitor treatment. Cells were treated with non-targeting siRNA control (NT) of with p21 siRNA (siCDKN1A) for 72 hours, after which cells were exposed to different concentrations of concentrations of AZD1775 (75, 150, 300 and 600 nM).*

To investigate the role of $p21^{Cip1/Waf1}$ in mediating AZD1775-induced cell death, both *SETD2* WT and *SETD2* KO U2OS cells were depleted of $p21^{Cip1/Waf1}$ using siRNA-interference treatment. In non-resistant *SETD2* WT and *SETD2* KO U2OS cell lines, both expressing low endogenous levels of cytoplasmic $p21^{Cip1/Waf1}$ (*Figure 3.11a*), downregulation of $p21^{Cip1/Waf1}$ resulted in a small, but significant, decrease in cell viability in response to WEE1 inhibitor treatment (*Figure 3.11b and c*).

3.9 Role of RRM2 in mediating AZD1775-resistance following knockdown of PAF1

Previous studies have shown that cytoplasmic $p21^{Cip1/Waf1}$ has additional functions besides inhibiting apoptosis via binding to procaspase 3, i.e. inhibition of the CDK2-cyclin A/B1/E and CDK1-cyclin A kinase activity and assembly of the D-type cyclins (D1, D2 and D3) with CDK4 and CDK6 (reviewed in Abbas & Dutta 2009). Activation of the CDK4/6-cyclin D complex helps to target Rb for phosphorylation, setting cells up for induction of broad transcriptional programs (see *Chapter 1.3.2 and 1.3.3*). Furthermore, inhibition of the CDK2-cyclin A and CDK1-cyclin A kinase is predicted to prevent Thr-33 phosphorylation of RRM2, thus reducing its ubiquitin-dependent protein degradation (see *Chapter 1.4.2.2*).

Therefore, it was hypothesized that PAF1 knockdown and subsequent localisation of $p21^{Cip1/Waf1}$ to the cytoplasm (*Figure 3.10a*) would increase RRM2 protein levels in both *SETD2* WT and *SETD2* KO U2OS cells in the presence of AZD1775. In order to confirm this, U2OS cells transfected with non-targeting control siRNA of PAF1 siRNA were treated with either DMSO (250 nM) or AZD1775 (250 nM) 48 hours post-transfection. Samples were then collected and levels of RRM2 were measured using Western Blot (*Figure 3.12*).

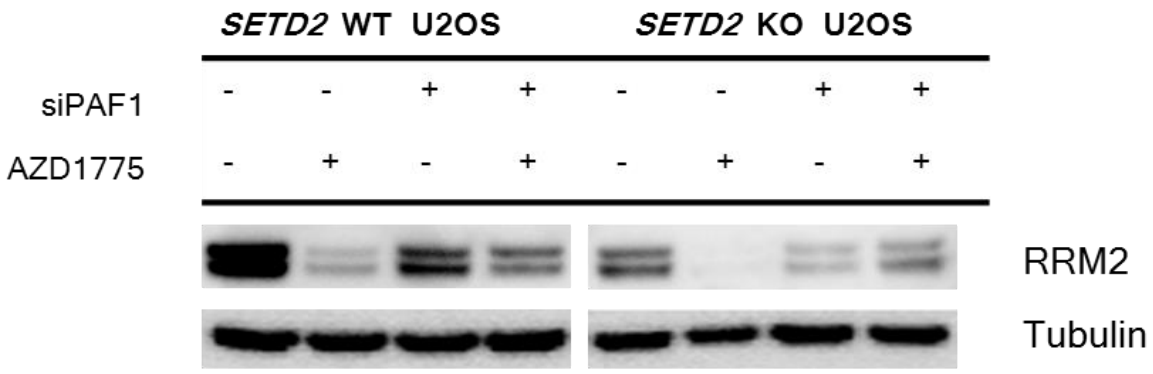

Figure 3.12. Analysis of RRM2 levels. *Western blot analysis of RRM2 protein levels in SETD2 WT and SETD2 CRISPR KO cells exposed to either non-targeting control siRNA or PAF1 siRNA and/or treated with either DMSO or 300 nM AZD1775. Tubulin was used as a loading control.*

As shown in *Figure 3.12*, RRM2 protein levels were strongly reduced following AZD1775 treatment (300 nM) in control siRNA treated *SETD2* WT U2OS cells. Moreover, AZD1775 treatment in *SETD2* KO U2OS cells further depleted RRM2 levels (*Figure 3.12*). Interestingly, however, knockdown of PAF1 suppressed the sensitivity of both *SETD2* WT and *SETD2* KO U2OS cells toward AZD1775 (*Figure 3.12*). Addition of AZD1775 in siPAF1-treated *SETD2* KO U2OS cells even resulted in a slight increase in RRM2 protein levels, suggesting that repletion of the dNTP pools via RRM2 upregulation might be one of the major determinants of PAF1-mediated resistance to AZD1775.

3.10 The Oct4/miR-106b pathway in regulating resistance to AZD1775 treatment

Finally, I tried to answer the question of how loss of PAF1 could result in enhanced localisation of $p21^{Cip1/Waf1}$ to the cytoplasm. A study by Ivanovska *et al.* has revealed that octamer-binding transcription factor 4 (Oct4) and a class of microRNAs belonging to the miR-106b seed family regulate cytoplasmic $p21^{Cip1/Waf1}$ expression and cell cycle progression (Ivanovska et al., 2008). It was therefore hypothesized that PAF1 mediates response to WEE1i treatment in both U2OS cells and RCC cell lines by modulating the Oct4/miR-106b/p21 pathway.

To start with, the expression levels of Oct4 were examined in both *SETD2* WT and *SETD2* KO U2OS cells as well as in the 786-O and A498 RCC cell lines (*Figure 3.13a*). Cortical neural stem cells (NSCs), known to spontaneously express the stem cell marker Oct4, were used as a positive control (*Figure 3.13a*).

The RCC cell lines 786-O and A498 show remarkably high levels of Oct4 (*Figure 3.13a*). Furthermore, it appeared as if SETD2(-/-) cell lines, including *SETD2* KO U2OS and A498, showed slightly lower levels of Oct4 when compared to SETD2(+/+) cell lines (*Figure 3.13a*).

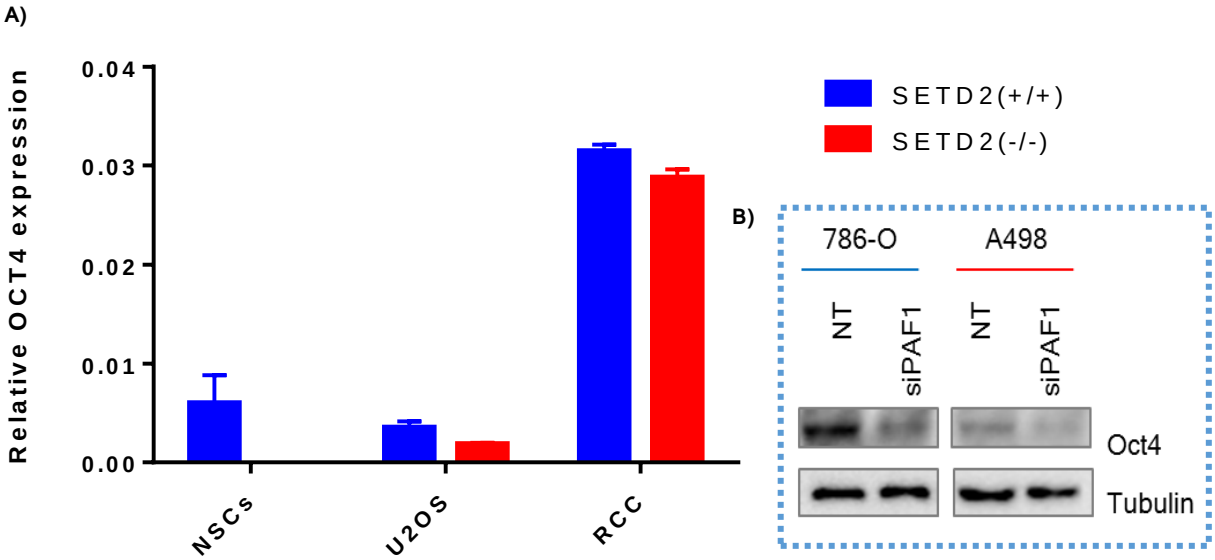

Figure 3.13. Analysis of Oct4 levels in renal cancer cell lines. A) *Analysis of POU5F1 (Oct4) mRNA levels in cortical neural stem cells, SETD2 WT U2OS cells, SETD2 CRISPR KO U2OS cells and renal cancer cell lines 786-O and A498 using RT-qPCR.* ***B)*** *Analysis of Oct4 protein levels. Protein extracts prepared from renal cancer cell lines 786-O and A498 72 hours after transfecction with PAF1 siRNA, and analysed by Western Blot with anti-Oct4 and anti-tubulin (loading control).*

To test whether PAF1 regulates Oct4 expression in kidney cancer, PAF1 was knocked-down in the renal cancer cell lines 786-O and A498, both expressing high levels of the pluripotency marker Oct4, with two independent siRNA pools. As shown in *Figure 3.13b,* levels of Oct4 strongly decreased in cells treated with PAF1 siRNA when compared to cells treated with non-targeting control siRNA.

As Oct4 has previously been found to regulate miR-106b-5p expression (Marson et al., 2008), I determined whether inhibition of miR-106b-5p could phenocopy the effect of PAF1 knockdown on cell viability in response to AZD1775 treatment. In order to do this, a synthetic hairpin inhibitor was used to specifically target miR-106b-5p in both *SETD2* WT and *SETD2* KO U2OS as well as in the 786-O and A498 RCC cell lines. The miRIDIAN microRNA Hairpin Inhibitor Negative Control #1 (Dharmacon) was used as a negative control.

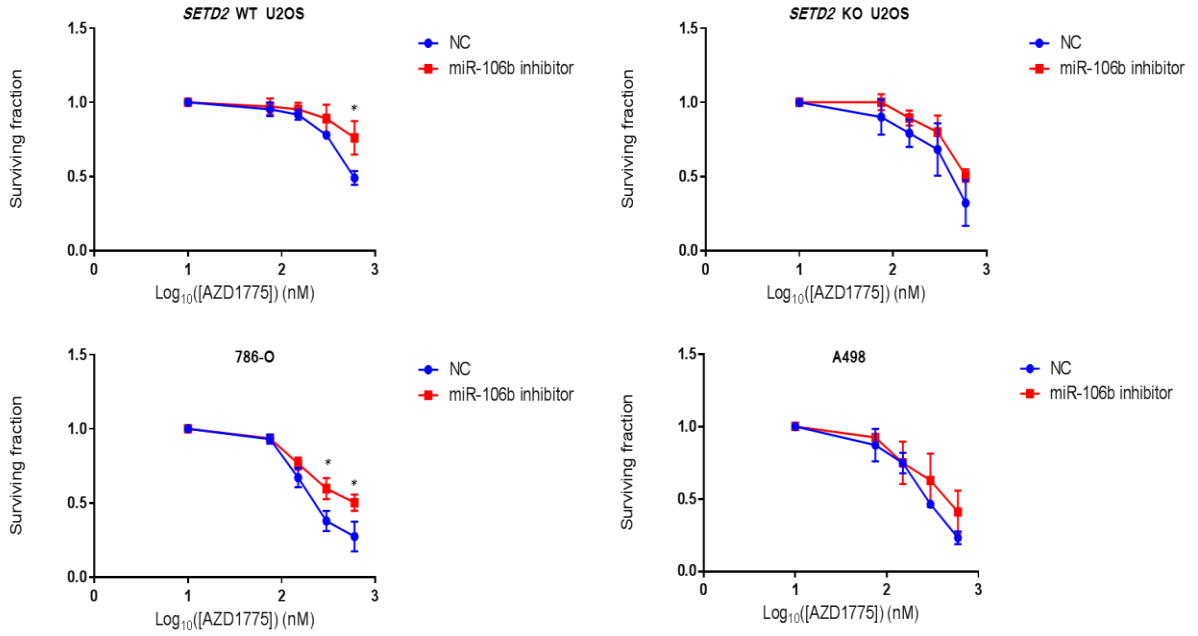

Figure 3.14. Role of miR-106b-5p in mediating AZD1775-induced cell death. *Survival fraction of miR-106b-5p hairpin inhibitor treated SETD2 WT U2OS, SETD2 CRISPR KO U2OS, 786-O and A498 cells after 72 h exposure to different concentrations of AZD1775 (75, 150, 300 and 600 nM). Data points and bars represent the mean and standard error of three independent experiments.*

As shown in *Figure 3.14*, it was found that inhibition of miR-106b-5p significantly blocked AZD1775-induced cell death both *SETD2* WT and 786-O renal cancer cells, mostly at higher concentrations of AZD1775. Those results suggest that PAF1 might partially response to WEE1i treatment by modulating the Oct4/miR-106b-5p pathway.

4 Chapter 4: General Discussion

The main aim of this study was to identify and characterise suppressors of the synthetic lethality resulting from loss of SETD2 and WEE1 in human cancer cells. This section summarises the major findings, discusses the possible mechanisms underlying resistance to WEE1 inhibitor treatment in H3K36me3-deficient cells, and considers the significance of those findings in a wider, more clinically relevant, context.

4.1 Summary

Using a genetic screen in fission yeast, we identified 23 mutants that suppressed the *set2Δ wee1-50* temperature sensitivity in *S. pombe*. Whole genome sequencing of these mutants followed by Gene Ontology term enrichment analysis revealed mutations in eight genes involved in cell cycle regulation (*bub1, cdc2, cut2, cut1, gtb1, myo52, slp1* and *wee1*), five genes involved in cell communication (*gpa1, shk1, ssp2, ste20* and *wis1*) and seven genes involved in transcription (*bdf1, brf1, bye1, epl1, lsm4, paf1* and *taf10*).

Further analysis in mammalian cells, as discussed in *Chapter 3*, showed that knockdown of spindle assembly checkpoint kinase BUB1 partially restored viability of *SETD2* CRISPR knock-out U2OS cells by maximal WEE1 inhibition. Additionally, it was found that knockdown of PAF1 partially rescued cell viability by higher concentrations (300 and 600 nM) of the WEE1 inhibitor AZD1775 in both *SETD2* WT and *SETD2* CRISPR knock-out U2OS cells. Data were later also verified in in RCC cell lines 786-O (*SETD2* wild-type) and A498 (bearing a truncating mutation in *SETD2*).

Investigations into the molecular mechanisms responsible for PAF1-mediated suppression suggested involvement of the CKI $p21^{Cip1/Waf1}$. Upon knockdown of PAF1 in both *SETD2* WT and *SETD2* KO U2OS cells, $p21^{Cip1/Waf1}$ expression was increased and it predominantly

relocalised from the nucleus to the cytoplasm. Cytoplasmic-localised $p21^{Cip1/Waf1}$ is thought to suppress the apoptotic response to WEE1i treatment by preventing the processing of caspase-3 as well as the degradation of RRM2 via CDK2 inhibition in the presence of AZD1775 (as measured by Western Blot). Analysis of the pathways responsible for regulation of SETD2 and $p21^{Cip1/Waf1}$ levels led to a proposed model whereby PAF1 dictates the response to AZD1775 via regulation of Oct4 and the miR-106b-5p seed family pathway, which in turn, regulates translation and subcellular localisation of $p21^{Cip1/Waf1}$ (for a diagrammatical representation of these findings, see *Figure 4.1*).

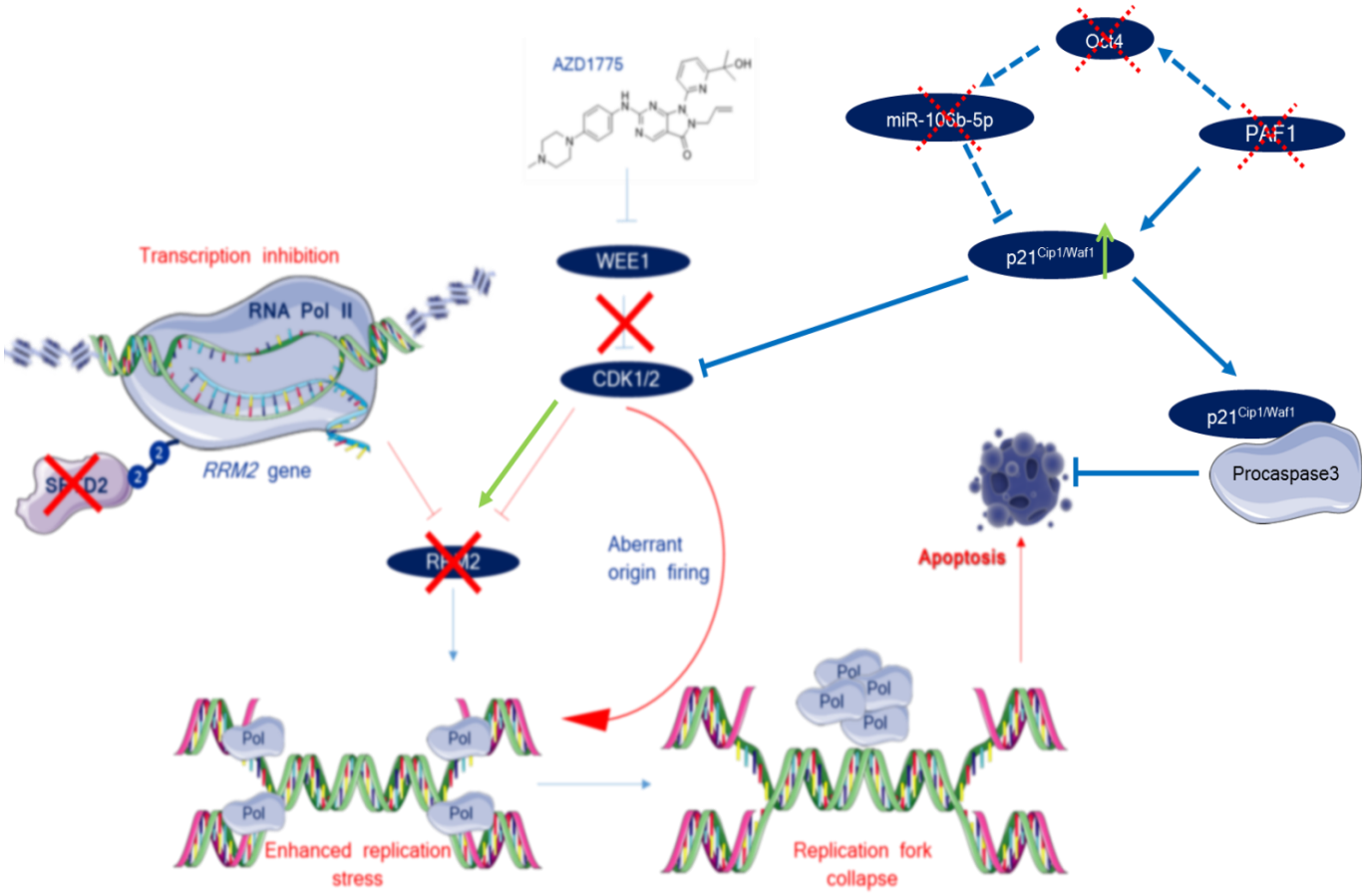

Figure 4.1. Model for WEE1i resistance in renal cell carcinoma cells. *The pluripotency factor Oct4 is highly expressed in renal cancer cell lines 786-O and A498. Following knock-down of PAF1, levels of Oct4 and miR-106b-5p are reduced. Decreased levels of miR-106b-5p subsequently enhance translation of* $p21^{Cip1/Waf1}$ *as well as promote shuffling of* $p21^{Cip1/Waf1}$ *from the nucleus towards the cytoplasm. Cytoplasmic-localised* $p21^{Cip1/Waf1}$ *might inhibit AZD1775-induced apoptosis via inhibition of caspase 3-cleavage as well as binding and subsequent inhibition of CDK2 kinase activity, thereby preventing degradation of RRM2.*

4.2 How does PAF1 silencing cause enhanced localisation of $p21^{cip1/waf1}$ to the cytoplasm?

Previous studies have shown that members of the PAF1 complex bind to the POU5F1 (Oct4) promoter in pluripotent embryonic stem cells, where they function to maintain a transcriptionally active chromatin structure (Ding et al., 2009). Data presented here suggest that the Paf1C promotes Oct4 expression not only during embryonic development but also during RCC tumourigenesis, as knockdown of PAF1 in 786-O and A498 renal cancer cells resulted in reduced levels of the key pluripotency marker Oct4. As Oct4 has recently been identified as an important transcriptional regulator for the miR-106b seed family (Marson et al., 2008), I tested whether inhibition of miR-106b-5p could phenocopy the effect of PAF1 knockdown on cell viability in response to AZD1775 treatment. Indeed, inhibition of miR-106b-5p also induced resistance to WEE1i treatment, mainly in *SETD2*-proficient cells, suggesting that PAF1 partially mediates response to AZD1775 via regulation of the Oct4/miR-106b-5p pathway.

In the context of resistance to WEE1i treatment, the miR-106b-5p family of microRNAs is particularly relevant as it is known to mediate two different pathways essential for AZD1775 response:

1) Firstly, lower levels of miR-106b have previously been associated with elevated protein expression of $p21^{Cip1/Waf1}$, as well as with enhanced localisation of $p21^{Cip1/Waf1}$ from the nucleus to the cytoplasm (Ivanovska et al., 2008; Kan et al., 2009; Koster et al., 2010). Cytoplasmic-localised $p21^{Cip1/Waf1}$, which was also found to be a major determinant in cisplatin-resistance in testicular cancer, can thereafter form a complex with the cyclin-dependent kinase CDK2, resulting in inhibition of its kinase activity (Koster et al., 2010). As CDK2 plays an important role in regulating sensitivity to WEE1i treatment (mainly because of its role in promoting origin firing and ubiquitin-mediated proteolysis of RRM2 upon hyper activation), inhibition of CDK2 kinase activity is hypothesised to be one of the main mediators of AZD1775-resistance following reduction of PAF1 and miR-106b-5p levels (see *Chapter 1.4.2.2*) (Pfister et al., 2015). This hypothesis is strongly supported by the finding that knockdown of PAF1 suppressed the sensitivity of both *SETD2* WT and *SETD2* CRISPR KO U2OS cells toward AZD1775 by suppressing degradation of RRM2.

2) Secondly, the methyltransferase SETD2 is a direct target of the microRNA seed family miR-106b (Xiang et al., 2015). Previous studies have shown that reduced levels of miR-106b-5p significantly up-regulated SETD2 protein levels by 4.4- to 7.5-fold in 786-O renal cancer cells (Xiang et al., 2015). As SETD2 is a major determinant of RRM2 expression (Pfister et al., 2015), upregulation of SETD2 levels due to lower levels of miR-106b-5p could replenish the nucleotide pools, leading to enhanced survival upon WEE1i treatment.

Even though enhanced localisation of $p21^{Cip1/Waf1}$ from the nucleus to the cytoplasm has been observed in response to PAF1 knockdown, cytoplasmic-localised $p21^{cip1/waf1}$ has not yet shown to be essential for WEE1i resistance in ccRCC. It would therefore be necessary to measure levels of cytoplasmic-$p21^{cip1/waf1}$ in AZD1775-resistant cancer tissues, as well as test whether those cells could then be re-sensitised to WEE1i treatment upon reduction and/or re-localisation of $p21^{cip1/waf1}$ to the nucleus.

4.3 Roles of RAF1-MEK-ERK1/2 and PI3K-AKT-mTOR pathways in mediating response to AZD1775-treatment

The RAF1-MEK-ERK1/2 cascade pathway, which can regulate transcription of various genes (e.g. c-Fos and c-Myc) involved in cell proliferation, survival, and motility upon activation, is thought to play an important role in the carcinogenesis of human RCCs (see *Chapter 1.1.2*). Constitutive activation of the mitogen-activated protein kinase kinase (MEK1/MAP2K1) as shown by the appearance of phosphorylated forms, was observed in more than half of high-grade human RCC cases when compared to controls (Oka et al., 1995). As hyper-activation of the RAF1-MEK-ERK1/2 signaling pathway has been shown to induce the expression of several CKIs, including $p21^{Cip1/Waf1}$, it was hypothesised that inhibition of MEK1 using siRNA or treatment with trametinib and/or selumetinib might modulate cell response to WEE1i treatment (Meloche & Pouysségur, 2007). However, as discussed in *Chapter* 3, siRNA mediated knockdown of MAP2K1/MEK1 did not have a significant effect on cell viability in response to WEE1i treatment. Those results further suggest that it is localisation

of $p21^{cip1/waf1}$ to the cytoplasm, and not necessarily increased $p21^{cip1/waf1}$ expression, that mediates resistance to AZD1775.

Another important pathway promoting proliferation, division, and cell survival when overexpressed in cancer is the phosphoinoside 3-kinase (PI3K)-mammalian target of rapamycin (mTOR) cascade. Loss of rapamycin complex 2 subunit *ste20* has previously been shown to strongly suppress the *set2*Δ *wee1-50* phenotype at non-permissive temperature (our unpublished data). Therefore, the role of the human ortholog RICTOR in mediating resistance to the lethality resulting from loss of SETD2 and WEE1 was further studied in mammalian cells. Viability of *SETD2* WT and *SETD2* CRISPR KO U2OS cells was however not significantly affected by RICTOR siRNA-interference treatment, suggesting that RICTOR in mammalian cells has distinct functions from *ste20* in *S. pombe*.

Even though RICTOR siRNA-interference treatment does not seem to affect the response of *SETD2* WT and *SETD2* CRISPR KO U2OS cells to WEE1i treatment, the PI3K-AKT-mTOR pathway might still be important in resistance to AZD1775 treatment. Recent studies have found that mTOR activation, as shown by sustained phosphorylation of pS6 (Ribosomal Protein)-S240/244 downstream target of the PI3K/mTOR pathway, is associated with AZD1775 resistance (Sen et al., 2017). Combination of AZD1775 with the allosteric mTORC1 inhibitor RAD001 significantly enhanced the cytotoxicity of WEE1 inhibition and subsequent apoptotic response when compared to treatment with AZD1775 alone, suggesting a role for mTORC1 rather than mTORC2 in mediating resistance to AZD1775 treatment (Sen et al., 2017).

4.4 Role of the spindle assembly checkpoint in mediating response to WEE1i-treatment

Following DNA damage, entry into mitosis is inhibited via the sensors ATM/ATR and their downstream targets checkpoint kinases 1 (Chk1) and 2 (Chk2), as described in *Chapter 1.3*

(Blackford & Jackson, 2017). Chk1 and Chk2 subsequently inactivate CDC25 and activate WEE1 kinase, thereby increasing the inhibitory tyrosine-15 phosphorylation in the ATP-binding domain of CDK1 (see *Chapter 1.3.5*) (reviewed by Kastan & Bartek 2004). Uncoupling of the DNA structure checkpoint at the G_2/M transition can however promote unscheduled activation of cyclin B1–CDK1, resulting in inappropriate entry into mitosis. To ensure that mitosis-incompetent cells, including those with under-replicated DNA and/or persistent DNA damage, are eliminated, cell death in mitosis – a process termed mitotic catastrophe – may be triggered (reviewed in Castedo et al., 2004).

Initial evidence for this came from studies with *S. pombe*, where it was demonstrated that the majority of *wee1-50* checkpoint deficient double mutants ultimately die at the restrictive temperature exhibiting a 'cut' (cell untimely torn) phenotype, consistent with cell death arising from mitotic catastrophe (Enoch, Carr, & Nurse, 1992). Recent evidence has emerged for *set2*Δ *wee1-50* double mutants, and even though most *set2*Δ *wee1-50* cells are thought to die from permanent replication stalling and subsequent S-phase catastrophe, another 30% does eventually appear to undergo mitotic catastrophe (our unpublished results). The *set2*Δ *wee1-50* synthetic lethality is highly conserved from fission yeast to humans, and although most H3K36me3-deficient cells have also been shown to undergo replication catastrophe following dNTP starvation and fork collapse (Pfister et al., 2015), a small number of cells might eventually complete S-phase and undergo mitotic catastrophe following G_2/M checkpoint abrogation.

Recently, it was found that cell death resulting from mitotic catastrophe can be inhibited by a number of factors, including partial impairment of SAC signalling, which ensures proper chromosome alignment before the onset of anaphase (see *Chapter 1.3.6*) (On, Chen, Ma, Chow, & Poon, 2011). As the spindle assembly checkpoint component serine/threonine-protein kinase Bub1 was identified in the suppressor screen in *S. pombe* (see *Chapter 3.1)*, I decided to test whether weakening of the SAC could help cells escape mitotic catastrophe (Taylor & McKeon,

1997) resulting from loss of SETD2 and WEE1. Indeed, we found that knockdown of human BUB1 significantly reduced sensitivity of *SETD2* CRISPR KO U2OS cells to higher concentrations of the WEE1 inhibitor. Previous studies have already shown that complete depletion of human BUB1 results in premature mitotic exit with an altered spindle rather than caspase-independent mitotic death and it could therefore be expected that the resistance to mitotic catastrophe observed in this study might be a result of a similar mechanism (Niikura, Dixit, Scott, Perkins, & Kitagawa, 2007) (for a diagrammatical representation of these findings, see *Figure 4.2*).

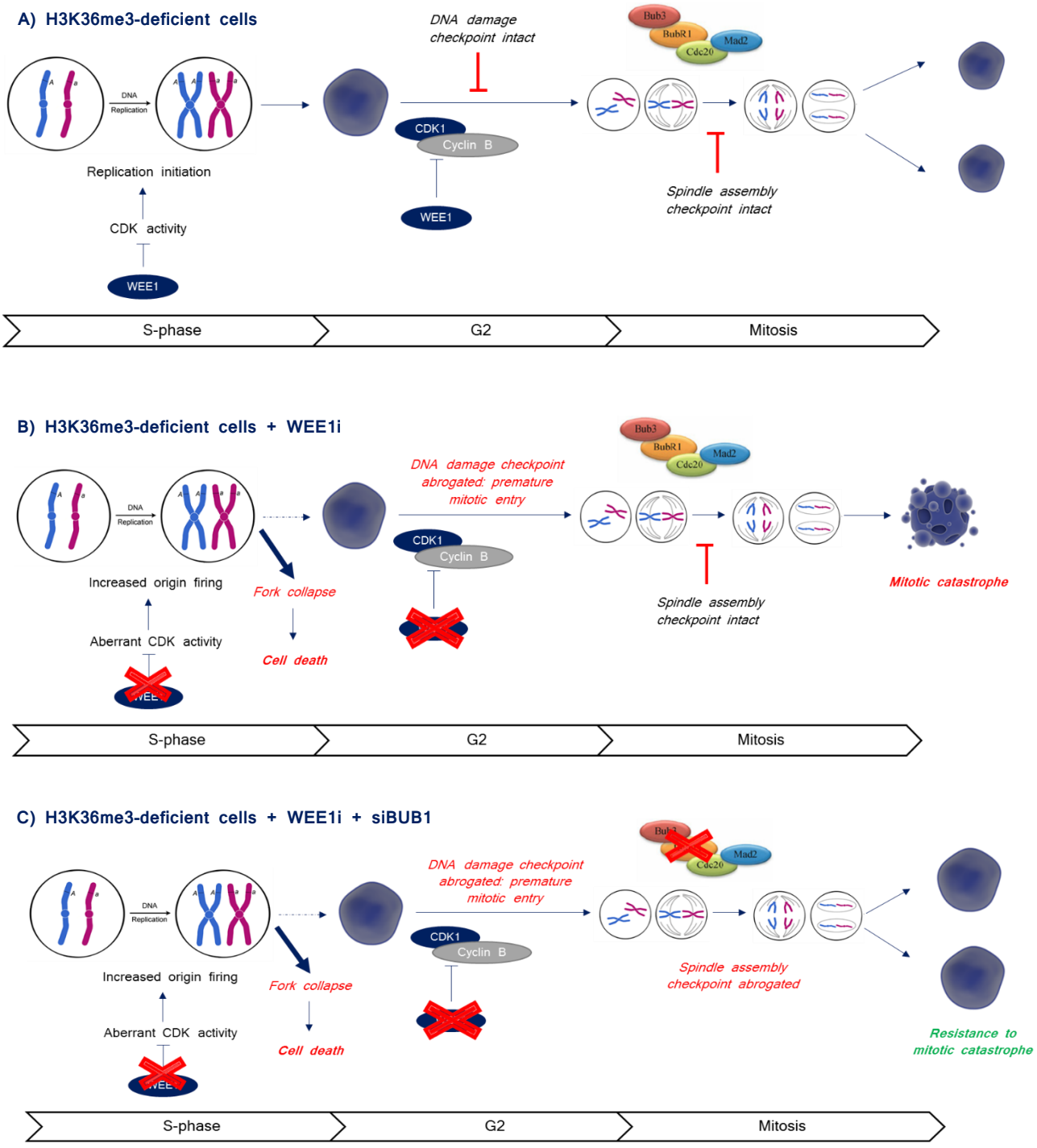

Figure 4.2. Model for BUB1-mediated resistance in renal cell carcinoma cells. A) Normal progression through the cell cycle. B) Progression through the cell cycle upon WEE1 inhibition. *Inactivation of WEE1 leads to dNTP pool depletion through increased firing of replication origins resulting from deregulated CDK activity. Most H3K36me3-deficient cells will consequently undergo apoptosis as a result of nucleotide shortage, fork collapse and replication catastrophe. A small percentage of cells might however escape replication catastrophe and will enter mitosis prematurely in the presence of damaged and under-replicated DNA due to G_2/M checkpoint abrogation. Remaining cells will therefore undergo segregation defects leading to mitotic catastrophe.* ***C) Progression through the cell cycle upon WEE1 inhibition and knockdown of BUB1.*** *Knockdown of the serine/threonine kinase BUB1 results in weakening of the spindle assembly checkpoint, inducing resistance to mitotic catastrophe in the small percentage of H3K36me3-deficient cells that has ultimately completed S-phase and entered mitosis.*

The finding that loss of BUB1 kinase only affects cell viability in response to WEE1 inhibition in *SETD2*-deficient cells but not in U2OS cells with functional SETD2, might have different explanations. Firstly, one explanation might be that SETD2-deficient cells are more dependent on activation of the SAC to maintain genome stability than cells with functional SETD2. Loss of SETD2 has been associated with reduced methylation of dynamic microtubules, causing mitotic spindle and cytokinesis defects, micronuclei, and polyploidy (Park et al., 2016) and activation of the SAC in SETD2-deficient cells might therefore be essential to eliminate cells lacking cytoskeletal integrity. Indeed, recent studies have shown that a number of genes participating in the metaphase checkpoint, including BUB1, AURKA and AURKB were overexpressed in a high percentage of CpG-island methylator phenotype (CIMP)-positive ccRCCs, including those that harbour mutations in and/or completely lack functional SETD2 (Arai et al., 2015; Tiedemann et al., 2016), suggesting that SAC integrity is important in those cell types. *SETD2* KO U2OS cells might therefore benefit more from weakening of the SAC and could consequently display resistance to mitotic catastrophe.

Secondly, different cell types have already been reported to display different susceptibilities to mitotic catastrophe and one of the major factors accounting for this is thought to be variation in mitotic time (On et al., 2011). There has been some preliminary evidence that loss of SETD2 causes defects in mitotic spindle and cytokinesis, subsequently resulting in mitosis time delay (Park et al., 2016). SETD2-knockout cells, which are believed to spend more time in mitosis, are therefore expected to be more susceptible to mitotic cell death (On et al., 2011), and could thus benefit more from the absence of a SAC.

4.5 Biological relevance of findings

Cell viability of H3K36me-3 deficient cells is suggested to be affected by effectiveness of SAC activation as loss of BUB1, which results in weakening or even complete abrogation of the SAC, appears to induce resistance to mitotic catastrophe. Among the potential mechanisms of acquired resistance to WEE1 inhibition, suppression of mitotic catastrophe is however not expected to cause major problems in clinical trials as cell death resulting from loss of SETD2 and WEE1 is still thought to be primarily caused by permanent replication stress and fork collapse (Pfister et al., 2015).

Furthermore, these findings reveal an important role for the Oct4/miR-106b-5p/p21 pathway in mediating resistance to WEE1i treatment in both SETD2-proficient and -deficient cancer cells. Recent studies have already demonstrated that expression levels of miR-106b are significantly lower in patients with advanced-stage RCC (Slaby et al., 2010) and this pathway could therefore be relevant for the escape of SETD2(-/-) cells from the inhibitory activity of AZD1775.

As cytoplasmic-localized $p21^{Cip1/Waf1}$ appears to be one of the main mediators of resistance to AZD1775-induced apoptosis, this could potentially be therapeutically targeted to prevent resistance from occurring. Previous studies have shown that phosphorylation of $p21^{cip1/waf1}$ at T145 by Akt enhances its cytoplasmic localisation (Zhou et al., 2001). PI3K/Akt inhibitors could therefore be used to re-localise $p21^{Cip1/Waf1}$ to the nucleus and could offer new strategies for treatment of AZD1775-resistant RCC and other types of cancer. Proof of concept for this approach has already been obtained in treatment of cisplatin-resistant testicular cancer cell lines, where treatment with the PI3K inhibitor LY294002 or the specific

Akt inhibitor triciribine resulted in dephosphorylation of Akt and concomitant dephosphorylation of p21 at T145, thereby causing re-localisation of $p21^{Cip1/Waf1}$ towards the nucleus (Koster et al., 2010). The more pronounced localisation of $p21^{Cip1/Waf1}$ in the nucleus resulted in reduced complex formation between $p21^{Cip1/Waf1}$ and CDK2, re-sensitizing resistant testicular embryonal carcinoma to cisplatin-induced apoptosis (Koster et al., 2010). If cytoplasmic-localised $p21^{cip1/waf1}$ does indeed turn out to be a major determinant in WEE1i-resistance in patients, combined therapy of PI3K/Akt inhibitors with AZD1775 could offer a promising approach to combat the adaptiveness of most tumours and possibly prevent the emergence of resistance.

Notably, a phase II clinical trial of the WEE1 inhibitor AZD1775 is about to start in patients with advanced refractory cancers harbouring amplification of the gene encoding cyclin E (CCNE1) (http://www.clinicaltrials.gov). Several studies have reported that tumours with deregulated cyclin E expression often display copy number loss, down-regulation and/or mutations in CDKN1A ($p21^{Cip1/Waf1}$) (Karst et al., 2014; Wiedemeyer et al., 2010; Xu et al., 2016). If CCNE-amplified tumour cells would indeed be sensitive to WEE1 inhibitor treatment as monotherapy, it would be very interesting to uncover whether a similar observation could be made for cancers that harbour CDKN1A copy number loss or mutation, as could be expected based on our own findings (*Figure 3.11).* Taken together, these studies could reveal whether Rb-E2F pathway activity is an important regulator of resistance to WEE1i treatment.

References

Abbas, T., & Dutta, A. (2009). p21 in cancer: intricate networks and multiple activities. *Nature Reviews. Cancer*, *9*(6), 400–14. https://doi.org/10.1038/nrc2657

Aktas, H., Cai, H., & Cooper, G. M. (1997). Ras links growth factor signaling to the cell cycle machinery via regulation of cyclin D1 and the Cdk inhibitor p27KIP1. *Molecular and Cellular Biology*, *17*(7), 3850–7. https://doi.org/10.1128/MCB.17.7.3850

Anda, S., Rothe, C., Boye, E., & Grallert, B. (2016). Consequences of abnormal CDK activity in S phase. *Cell Cycle*, *15*(7), 963–973. https://doi.org/10.1080/15384101.2016.1152423

Arai, E., Gotoh, M., Tian, Y., Sakamoto, H., Ono, M., Matsuda, A., … Kanai, Y. (2015). Alterations of the spindle checkpoint pathway in clinicopathologically aggressive CpG island methylator phenotype clear cell renal cell carcinomas. *International Journal of Cancer*, *137*(11), 2589–2606. https://doi.org/10.1002/ijc.29630

Arya, G., & Schlick, T. (2009). A tale of tails: how histone tails mediate chromatin compaction in different salt and linker histone environments. *Journal of Physical Chemistry A*, *113*(16), 4045–4059. https://doi.org/10.1021/jp810375d

Ashworth, A. (2008). A synthetic lethal therapeutic approach: Poly(ADP) ribose polymerase inhibitors for the treatment of cancers deficient in DNA double-strand break repair. *Journal of Clinical Oncology*. https://doi.org/10.1200/JCO.2008.16.0812

Aymard, F., Bugler, B., Schmidt, C. K., Guillou, E., Caron, P., Briois, S., … Legube, G. (2014). Transcriptionally active chromatin recruits homologous recombination at DNA double-strand breaks. *Nature Structural & Molecular Biology*, *21*(4), 366–74. https://doi.org/10.1038/nsmb.2796

Baldin, V., Lukas, J., Marcote, M. J., Pagano, M., & Draetta, G. (1993). Cyclin D1 is a nuclear protein required for cell cycle progression in G1. *Genes Dev*, *7*(5), 812–821. https://doi.org/10.1101/gad.7.5.812

Bannister, A. J., Schneider, R., Myers, F. A., Thorne, A. W., Crane-Robinson, C., & Kouzarides, T. (2005). Spatial distribution of di- and tri-methyl lysine 36 of histone H3 at active genes. *Journal of Biological Chemistry*, *280*(18), 17732–17736. https://doi.org/10.1074/jbc.M500796200

Baubec, T., Colombo, D. F., Wirbelauer, C., Schmidt, J., Burger, L., Krebs, A. R., … Schu, D. (2015). Genomic profilingofDNAmethyltransferases reveals a role for DNMT3B in genic methylation. *Nature*, *520*(7546), 243–7. https://doi.org/10.1038/nature14176

Beck, H., Nahse-Kumpf, V., Larsen, M. S. Y., O'Hanlon, K. A., Patzke, S., Holmberg, C., … Sorensen, C. S. (2012). Cyclin-Dependent Kinase Suppression by WEE1 Kinase Protects the Genome through Control of Replication Initiation and Nucleotide Consumption. *Molecular and Cellular Biology*, *32*(20), 4226–4236. https://doi.org/10.1128/MCB.00412-12

Besson, A., Dowdy, S. F., & Roberts, J. M. (2008). CDK Inhibitors: Cell Cycle Regulators and Beyond. *Developmental Cell*. https://doi.org/10.1016/j.devcel.2008.01.013

Black, J. C., Van Rechem, C., & Whetstine, J. R. (2012). Histone Lysine Methylation Dynamics: Establishment, Regulation, and Biological Impact. *Molecular Cell*. https://doi.org/10.1016/j.molcel.2012.11.006

Blackford, A. N., & Jackson, S. P. (2017). ATM, ATR, and DNA-PK: The Trinity at the Heart of the DNA Damage Response. *Molecular Cell*. https://doi.org/10.1016/j.molcel.2017.05.015

Booher, R. N., Holman, P. S., & Fattaey, A. (1997). Human Myt1 is a cell cycle-regulated kinase that inhibits Cdc2 but not Cdk2 activity. *Journal of Biological Chemistry*, *272*(35), 22300–22306. https://doi.org/10.1074/jbc.272.35.22300

Braden, W. A., McClendon, A. K., & Knudsen, E. S. (2008). Cyclin-dependent kinase 4/6 activity is a critical determinant of pre-replication complex assembly. *Oncogene*, *27*(56), 7083–7093. https://doi.org/10.1038/onc.2008.319

Bryant, H. E., Schultz, N., Thomas, H. D., Parker, K. M., Flower, D., Lopez, E., … Helleday, T. (2005). Specific killing of BRCA2-deficient tumours with inhibitors of poly(ADP-ribose) polymerase. *Nature*, *434*(7035), 913–917. https://doi.org/10.1038/nature03443

Cancer Genome Atlas Research Network. (2013). Comprehensive molecular characterization of clear cell renal cell carcinoma. *Nature*, *499*(7456), 43–49. https://doi.org/10.1038/nature12222

Capitanio, U., Cloutier, V., Zini, L., Isbarn, H., Jeldres, C., Shariat, S. F., … Karakiewicz, P. I. (2009). A critical assessment of the prognostic value of clear cell, papillary and chromophobe histological subtypes in renal cell carcinoma: A population-based study. *BJU International*, *103*(11), 1496–1500.

https://doi.org/10.1111/j.1464-410X.2008.08259.x

Carvalho, S., Raposo, A. C., Martins, F. B., Grosso, A. R., Sridhara, S. C., Rino, J., … De Almeida, S. F. (2013). Histone methyltransferase SETD2 coordinates FACT recruitment with nucleosome dynamics during transcription. *Nucleic Acids Research*, *41*(5), 2881–2893. https://doi.org/10.1093/nar/gks1472

Carvalho, S., Vítor, A. C., Sridhara, S. C., Filipa, B. M., Ana, C. R., Desterro, J. M. P., … de Almeida, S. F. (2014). SETD2 is required for DNA double-strand break repair and activation of the p53-mediated checkpoint. *eLife*, *2014*(3), 1–19. https://doi.org/10.7554/eLife.02482

Castedo, M., Perfettini, J.-L., Roumier, T., Andreau, K., Medema, R., & Kroemer, G. (2004). Cell death by mitotic catastrophe: a molecular definition. *Oncogene*, *23*(16), 2825–37. https://doi.org/10.1038/sj.onc.1207528

Coleman, T. R., & Dunphy, W. G. (1994). Cdc2 regulatory factors. *Current Opinion in Cell Biology*, *6*(6), 877–882. https://doi.org/10.1016/0955-0674(94)90060-4

Cooper, G. M., & Hausman, R. E. (2007). *The Cell: A Molecular Approach 2nd Edition*. *Sinauer Associates*.

Coverley, D., Laman, H., & Laskey, R. A. (2002). Distinct roles for cyclins E and A during DNA replication complex assembly and activation. *Nature Cell Biology*, *4*(7), 523–528. https://doi.org/10.1038/ncb813

D'Angiolella, V., Donato, V., Forrester, F. M., Jeong, Y. T., Pellacani, C., Kudo, Y., … Pagano, M. (2012). Cyclin F-mediated degradation of ribonucleotide reductase M2 controls genome integrity and DNA repair. *Cell*, *149*(5), 1023–1034. https://doi.org/10.1016/j.cell.2012.03.043

Dalgliesh, G. L., Furge, K., Greenman, C., Chen, L., Bignell, G., Butler, A., … Futreal, P. A. (2010). Systematic sequencing of renal carcinoma reveals inactivation of histone modifying genes. *Nature*, *463*(7279), 360–363. https://doi.org/10.1038/nature08672

Daugaard, M., Baude, A., Fugger, K., Povlsen, L. K., Beck, H., Sørensen, C. S., … Jäättelä, M. (2012). LEDGF (p75) promotes DNA-end resection and homologous recombination. *Nature Structural & Molecular Biology*, *19*(8), 803–810. https://doi.org/10.1038/nsmb.2314

Ding, L., Paszkowski-Rogacz, M., Nitzsche, A., Slabicki, M. M., Heninger, A. K., Vries, I. de, … Buchholz, F. (2009). A Genome-Scale RNAi Screen for Oct4 Modulators Defines a Role of the Paf1 Complex for Embryonic Stem Cell Identity. *Cell Stem Cell*, *4*(5), 403–415. https://doi.org/10.1016/j.stem.2009.03.009

Duns, G., van den Berg, E., van Duivenbode, I., Osinga, J., Hollema, H., Hofstra, R. M. W., & Kok, K. (2010). Histone methyltransferase gene SETD2 is a novel tumor suppressor gene in clear cell renal cell carcinoma. *Cancer Research*, *70*(11), 4287–4291. https://doi.org/10.1158/0008-5472.CAN-10-0120

Edmunds, J. W., Mahadevan, L. C., & Clayton, A. L. (2008). Dynamic histone H3 methylation during gene induction: HYPB/Setd2 mediates all H3K36 trimethylation. *The EMBO Journal*, *27*, 406–420. https://doi.org/10.1038/

Elledge, S. J., Zhou, Z., & Allen, J. B. (1992). Ribonucleotide reductase: regulation, regulation, regulation. *Trends in Biochemical Sciences*, *17*(3), 119–123. https://doi.org/10.1016/0968-0004(92)90249-9

Enoch, T., Carr, A. M., & Nurse, P. (1992). Fission yeast genes involved in coupling mitosis to completion of DNA replication. *Genes and Development*, *6*(11), 2035–2046. https://doi.org/10.1101/gad.6.11.2035

Ewen, M. E., Sluss, H. K., Sherr, C. J., Matsushime, H., Kato, J., & Livingston, D. M. (1993). Functional interactions of the retinoblastoma protein with mammalian D- type cyclins. *Cell*, *73*(3), 487–497.

Farmer, H., McCabe, N., Lord, C. J., Tutt, A. N. J., Johnson, D. A., Richardson, T. B., … Ashworth, A. (2005). Targeting the DNA repair defect in BRCA mutant cells as a therapeutic strategy. *Nature*, *434*(7035), 917–921. https://doi.org/10.1038/nature03445

Ferlay, J., Soerjomataram, I., Ervik, M., Dikshit, R., Eser, S., Mathers, C., … Bray, F. (2013). GLOBOCAN 2012 v1.0, Cancer Incidence and Mortality Worldwide: IARC CancerBase. No. 11 [Internet]. https://doi.org/10.1016/j.ucl.2013.01.011

Geng, Y., Eaton, E. N., Picón, M., Roberts, J. M., Lundberg, A. S., Gifford, A., … Weinberg, R. A. (1996). Regulation of cyclin E transcription by E2Fs and retinoblastoma protein. *Oncogene*, *12*(6), 1173–1180.

Gerlinger, M., Rowan, A. J., Horswell, S., Larkin, J., Endesfelder, D., Gronroos, E., … Swanton, C. (2012). Intratumor heterogeneity and branched evolution revealed by multiregion sequencing. *The New England Journal of Medicine*, *366*(10), 883–92. https://doi.org/10.1056/NEJMoa1113205

Groenendijk, F. H., & Bernards, R. (2014). Drug resistance to targeted therapies: Déjà vu all over again. *Molecular Oncology*. https://doi.org/10.1016/j.molonc.2014.05.004

Guarente, L. (1993). Synthetic enhancement in gene interaction: a genetic tool come of age. *Trends in Genetics*, *9*(10), 362–366. https://doi.org/10.1016/0168-9525(93)90042-G

Hakimi, A. A., Chen, Y. B., Wren, J., Gonen, M., Abdel-Wahab, O., Heguy, A., … Hsieh, J. J. (2013). Clinical and pathologic impact of select chromatin-modulating tumor suppressors in clear cell renal cell carcinoma. *Eur Urol*, *63*(5), 848–854. https://doi.org/10.1016/j.eururo.2012.09.005

Hakimi, A. A., Ostrovnaya, I., Reva, B., Schultz, N., Chen, Y. B., Gonen, M., … Hsieh, J. J. (2013). Adverse outcomes in clear cell renal cell carcinoma with mutations of 3p21 epigenetic regulators BAP1 and SETD2: A report by MSKCC and the KIRC TCGA research network. *Clinical Cancer Research*, *19*(12), 3259–3267. https://doi.org/10.1158/1078-0432.CCR-12-3886

Hanahan, D., & Weinberg, R. A. (2000). The hallmarks of cancer. *Cell*, *100*(1), 57–70. https://doi.org/10.1007/s00262-010-0968-0

Hanahan, D., & Weinberg, R. A. (2011). Hallmarks of cancer: The next generation. *Cell*. https://doi.org/10.1016/j.cell.2011.02.013

Harbour, J. W., Luo, R. X., Dei Santi, A., Postigo, A. A., & Dean, D. C. (1999). Cdk phosphorylation triggers sequential intramolecular interactions that progressively block Rb functions as cells move through G1. *Cell*, *98*(6), 859–869. https://doi.org/10.1016/S0092-8674(00)81519-6

Harper, J. V, & Brooks, G. (2004). The Mammalian Cell Cycle. In *Cell Cycle Control: Mechanisms and Protocols* (Vol. 296, pp. 113–153). https://doi.org/10.1385/1-59259-857-9:113

Hartwell, L., & Weinert, T. (1989). Checkpoints: controls that ensure the order of cell cycle events. *Science*, *246*(4930), 629–634. https://doi.org/10.1126/science.2683079

Ho, T. H., Park, I. Y., Zhao, H., Tong, P., Champion, M. D., Yan, H., … Jonasch, E. (2015). High-resolution profiling of histone h3 lysine 36 trimethylation in metastatic renal cell carcinoma. *Oncogene*, (August 2014), 1–10. https://doi.org/10.1038/onc.2015.221

Horn, P. J., & Peterson, C. L. (2002). Chromatin higher order folding: wrapping up transcription. *Science*, *297*(5588), 1824–1827. https://doi.org/10.1126/science.1074200

Horvath, J. E., Bailey, J. a, Locke, D. P., & Eichler, E. E. (2001). Lessons from the human genome: transitions between euchromatin and heterochromatin. *Human Molecular Genetics*, *10*(20), 2215–2223. https://doi.org/10.1093/hmg/10.20.2215

Iliopoulos, O., Levy, a P., Jiang, C., Kaelin, W. G., & Goldberg, M. a. (1996). Negative regulation of hypoxia-

inducible genes by the von Hippel-Lindau protein. *Proceedings of the National Academy of Sciences of the United States of America*, *93*(20), 10595–10599. https://doi.org/10.1073/pnas.93.20.10595

Inaba, T., Matsushime, H., Valentine, M., Roussel, M. F., Sherr, C. J., & Look, A. T. (1992). Genomic organization, chromosomal localization, and independent expression of human cyclin D genes. *Genomics*, *13*(3), 565–574. https://doi.org/10.1016/0888-7543(92)90126-D

Ivanovska, I., Ball, A. S., Diaz, R. L., Magnus, J. F., Kibukawa, M., Schelter, J. M., … Cleary, M. A. (2008). MicroRNAs in the miR-106b Family Regulate p21/CDKN1A and Promote Cell Cycle Progression. *Molecular and Cellular Biology*, *28*(7), 2167–2174. https://doi.org/10.1128/MCB.01977-07

Jenuwein, T., Laible, G., Dorn, R., & Reuter, G. (1998). SET domain proteins modulate chromatin domains in eu- and heterochromatin. *Cellular and Molecular Life Sciences*. https://doi.org/10.1007/s000180050127

Jia, L., Li, B., & Yu, H. (2016). The Bub1-Plk1 kinase complex promotes spindle checkpoint signalling through Cdc20 phosphorylation. *Nature Communications*, *7*, 10818. https://doi.org/10.1038/ncomms10818

Jiang, C., & Pugh, B. F. (2009). Nucleosome positioning and gene regulation: advances through genomics. *Nature Reviews Genetics*, *10*(3), 161–172. https://doi.org/10.1038/nrg2522

Johnson, D. G., & Schneider-Broussard, R. (1998). Role of E2F in cell cycle control and cancer. *Front Biosci*, *3*, d447-8.

Kan, T., Sato, F., Ito, T., Matsumura, N., David, S., Cheng, Y., … Meltzer, S. J. (2009). The miR-106b-25 Polycistron, Activated by Genomic Amplification, Functions as an Oncogene by Suppressing p21 and Bim. *Gastroenterology*, *136*(5), 1689–1700. https://doi.org/10.1053/j.gastro.2009.02.002

Karst, A. M., Jones, P. M., Vena, N., Ligon, A. H., Liu, J. F., Hirsch, M. S., … Drapkin, R. (2014). Cyclin E1 deregulation occurs early in secretory cell transformation to promote formation of fallopian tube-derived high-grade serous ovarian cancers. *Cancer Research*, *74*(4), 1141–1152. https://doi.org/10.1158/0008-5472.CAN-13-2247

Kastan, M. B., & Bartek, J. (2004). Cell-cycle checkpoints and cancer. *Nature*, *432*(7015), 316–323. https://doi.org/10.1038/nature03097

Keegan, K. A., Schupp, C. W., Chamie, K., Hellenthal, N. J., Evans, C. P., & Koppie, T. M. (2012). Histopathology of surgically treated renal cell carcinoma: Survival differences by subtype and stage.

Journal of Urology, *188*(2), 391–397. https://doi.org/10.1016/j.juro.2012.04.006

Kizer, K. O., Phatnani, H. P., Shibata, Y., Hall, H., Greenleaf, A. L., & Strahl, B. D. (2005). A Novel Domain in Set2 Mediates RNA Polymerase II Interaction and Couples Histone H3 K36 Methylation with Transcript Elongation. *Molecular and Cellular Biology*, *25*(8), 3305–3316. https://doi.org/10.1128/MCB.25.8.3305-3316.2005

Kolasinska-Zwierz, P., Down, T., Latorre, I., Liu, T., Liu, X. S., & Ahringer, J. (2009). Differential chromatin marking of introns and expressed exons by H3K36me3. *Nature Genetics*, *41*(3), 376–381. https://doi.org/10.1038/ng.322.Differential

Koster, R., Pietro, A., Timmer-Bosscha, H., Gibcus, J. H., Berg, A. Van Den, Suurmeijer, A. J., … Jong, S. De. (2010). Cytoplasmic p21 expression levels determine cisplatin resistance in human testicular cancer. *The Journal of Clinical Investigation*, *120*(10), 3594–605. https://doi.org/10.1172/JCI41939DS1

Lam, J. S., Leppert, J. T., Belldegrun, A. S., & Figlin, R. A. (2005). Novel approaches in the therapy of metastatic renal cell carcinoma. *World Journal of Urology*. https://doi.org/10.1007/s00345-004-0466-0

Lara-Gonzalez, P., Westhorpe, F. G., & Taylor, S. S. (2012). The spindle assembly checkpoint. *Current Biology*. https://doi.org/10.1016/j.cub.2012.10.006

Latif, F., Tory, K., Gnarra, J., Yao, M., Duh, F., Orcutt, M., … et, al. (1993). Identification of the von Hippel-Lindau disease tumor suppressor gene. *Science*, *260*(5112), 1317–1320. https://doi.org/10.1126/science.8493574

Li, B., Howe, L., Anderson, S., Yates, J. R., & Workman, J. L. (2003). The Set2 histone methyltransferase functions through the phosphorylated carboxyl-terminal domain of RNA polymerase II. *The Journal of Biological Chemistry*, *278*(11), 8897–903. https://doi.org/10.1074/jbc.M212134200

Li, F., Mao, G., Tong, D., Huang, J., Gu, L., Yang, W., & Li, G. M. (2013). The histone mark H3K36me3 regulates human DNA mismatch repair through its interaction with MutSα. *Cell*, *153*(3), 590–600. https://doi.org/10.1016/j.cell.2013.03.025

Ljungberg, B., Bensalah, K., Canfield, S., Dabestani, S., Hofmann, F., Hora, M., … Bex, A. (2015). EAU guidelines on renal cell carcinoma: 2014 update. *European Urology*. https://doi.org/10.1016/j.eururo.2015.01.005

Ljungberg Bensalah, K., Bex, A., Canfield, S., Dabestani, S., Hofmann, F., Hora, M., Kuczyk M.A., Lam, T., Marconi, L., Merseburger, A.S., Mulders, P.F.A., Staehler, M., Volpe, A., B. (2016). Guidelines on Renal Cell Carcinoma, (European Association of Urology).

Lopez-Beltran, A., Scarpelli, M., Montironi, R., & Kirkali, Z. (2006). 2004 WHO Classification of the Renal Tumors of the Adults. *European Urology*. https://doi.org/10.1016/j.eururo.2005.11.035

Luco, R. F., Pan, Q., Tominaga, K., Blencowe, B. J., Pereira-Smith, O. M., & Misteli, T. (2010). Regulation of alternative splicing by histone modifications. *Science (New York, N.Y.)*, *327*(5968), 996–1000. https://doi.org/10.1126/science.1184208

Luger, K., Mäder, A. W., Richmond, R. K., Sargent, D. F., & Richmond, T. J. (1997). Crystal structure of the nucleosome core particle at 2.8 A resolution. *Nature*, *389*(6648), 251–60. https://doi.org/10.1038/38444

Lundberg, A. S., & Weinberg, R. A. (1998). Functional Inactivation of the Retinoblastoma Protein Requires Sequential Modification by at Least Two Distinct Cyclin-cdk Complexes. *Molecular and Cellular Biology*, *18*(2), 753–761. https://doi.org/10.1128/MCB.18.2.753

Marson, A., Levine, S. S., Cole, M. F., Frampton, G. M., Brambrink, T., Johnstone, S., … Young, R. A. (2008). Connecting microRNA Genes to the Core Transcriptional Regulatory Circuitry of Embryonic Stem Cells. *Cell*, *134*(3), 521–533. https://doi.org/10.1016/j.cell.2008.07.020

Martinez, a, Fullwood, P., Kondo, K., Kishida, T., Yao, M., Maher, E. R., & Latif, F. (2000). Role of chromosome 3p12-p21 tumour suppressor genes in clear cell renal cell carcinoma: analysis of VHL dependent and VHL independent pathways of tumorigenesis. *Molecular Pathology : MP*, *53*(3), 137–44. https://doi.org/10.1136/mp.53.3.137

Matheson, C. J., Backos, D. S., & Reigan, P. (2016). Targeting WEE1 Kinase in Cancer. *Trends in Pharmacological Sciences*. https://doi.org/10.1016/j.tips.2016.06.006

Matheson, C. J., Venkataraman, S., Amani, V., Harris, P. S., Backos, D. S., Donson, A. M., … Reigan, P. (2016). A WEE1 Inhibitor Analog of AZD1775 Maintains Synergy with Cisplatin and Demonstrates Reduced Single-Agent Cytotoxicity in Medulloblastoma Cells. *ACS Chemical Biology*, *11*(4), 921–930. https://doi.org/10.1021/acschembio.5b00725

Matsushime, H., Quelle, D. E., Shurtleff, S. a, Shibuya, M., Sherr, C. J., & Kato, J. Y. (1994). D-type cyclin-

dependent kinase activity in mammalian cells. *Molecular and Cellular Biology*, *14*(3), 2066–76. https://doi.org/10.1128/MCB.14.3.2066.Updated

Maxwell, P. H., Wiesener, M. S., Chang, G. W., Clifford, S. C., Vaux, E. C., Cockman, M. E., … Ratcliffe, P. J. (1999). The tumour suppressor protein VHL targets hypoxia-inducible factors for oxygen-dependent proteolysis. *Nature*, *399*(6733), 271–275. https://doi.org/10.1038/20459

Meloche, S., & Pouysségur, J. (2007). The ERK1/2 mitogen-activated protein kinase pathway as a master regulator of the G1- to S-phase transition. *Oncogene*, *26*(22), 3227–39. https://doi.org/10.1038/sj.onc.1210414

Méndez, J., & Stillman, B. (2000). Chromatin association of human origin recognition complex, cdc6, and minichromosome maintenance proteins during the cell cycle: assembly of prereplication complexes in late mitosis. *Molecular and Cellular Biology*, *20*(22), 8602–12. https://doi.org/10.1128/MCB.20.22.8602-8612.2000.

Meyerson, M., & Harlow, E. (1994). Identification of G1 kinase activity for cdk6, a novel cyclin D partner. *Molecular and Cellular Biology*, *14*(3), 2077–86. https://doi.org/10.1128/MCB.14.3.2077.Updated

Mickisch, G. H. (1994). Chemoresistance of renal cell carcinoma: 1986-1994. *World Journal of Urology*, *12*(4), 214–223. https://doi.org/10.1007/BF00185677

Moreno, S., Klar, A., & Nurse, P. (1991). [56] Molecular genetic analysis of fission yeast Schizosaccharomyces pombe. *Methods in Enzymology*, *194*, 795–823. https://doi.org/10.1016/0076-6879(91)94059-L

Morgan, D. O. (1995). Principles of CDK regulation. *Nature*, *374*(6518), 131–134. https://doi.org/10.1038/374131a0

Motokura, T., Keyomarsi, K., Kronenberg, H. M., & Arnold, A. (1992). Cloning and Characterization of Human Cyclin D3, a Cdna Closely Related in Sequence to the Prad1 Cyclin-D1 Protooncogene. *Journal of Biological Chemistry*, *267*(28), 20412–20415.

Musselman, C. A., Khorasanizadeh, S., & Kutateladze, T. G. (2014). Towards understanding methyllysine readout. *Biochimica et Biophysica Acta - Gene Regulatory Mechanisms*. https://doi.org/10.1016/j.bbagrm.2014.04.001

Neri, F., Rapelli, S., Krepelova, A., Incarnato, D., Parlato, C., Basile, G., … Oliviero, S. (2017). Intragenic

DNA methylation prevents spurious transcription initiation. *Nature*. https://doi.org/10.1038/nature21373

Niikura, Y., Dixit, A., Scott, R., Perkins, G., & Kitagawa, K. (2007). BUB1 mediation of caspase-independent mitotic death determines cell fate. *Journal of Cell Biology*, *178*(2), 283–296. https://doi.org/10.1083/jcb.200702134

Oka, H., Chatani, Y., Hoshino, R., Ogawa, O., Kakehi, Y., Terachi, T., … Yoshida, O. (1995). Constitutive activation of mitogen-activated protein (MAP) kinases in human renal cell carcinoma. *Cancer Res*, *55*(18), 4182–4187.

On, K. F., Chen, Y., Ma, H. T., Chow, J. P. H., & Poon, R. Y. C. (2011). Determinants of mitotic catastrophe on abrogation of the G2 DNA damage checkpoint by UCN-01. *Molecular Cancer Therapeutics*, *10*(5), 784–794. https://doi.org/10.1158/1535-7163.MCT-10-0809

Ortega, S., Malumbres, M., & Barbacid, M. (2002). Cyclin D-dependent kinases, INK4 inhibitors and cancer. *Biochimica et Biophysica Acta - Reviews on Cancer*. https://doi.org/10.1016/S0304-419X(02)00037-9

Otto, T., & Sicinski, P. (2017). Cell cycle proteins as promising targets in cancer therapy. *Nature Reviews Cancer*, *17*(2), 93–115. https://doi.org/10.1038/nrc.2016.138

Pagano, M., Pepperkok, R., Lukas, J., Baldin, V., Ansorge, W., Bartek, J., & Draetta, G. (1993). Regulation of the cell cycle by the cdk2 protein kinase in cultured human fibroblasts. *The Journal of Cell Biology*, *121*(1), 101–111.

Pardee, a B. (1974). A restriction point for control of normal animal cell proliferation. *Proceedings of the National Academy of Sciences of the United States of America*, *71*(4), 1286–90. https://doi.org/10.1073/pnas.71.4.1286

Park, I. Y., Powell, R. T., Tripathi, D. N., Dere, R., Ho, T. H., Blasius, T. L., … Walker, C. L. (2016). Dual Chromatin and Cytoskeletal Remodeling by SETD2. *Cell*, *166*(4), 950–962. https://doi.org/10.1016/j.cell.2016.07.005

Parker, L. L., & Piwnica-Worms, H. (1992). Inactivation of the p34cdc2-Cyclin B Complex by the Human WEE1 Tyrosine Kinase. *Science*, *257*(1989), 1955–1957. https://doi.org/10.1126/science.1384126

Pfister, S. X., Ahrabi, S., Zalmas, L. P., Sarkar, S., Aymard, F., Bachrati, C. Z., … Humphrey, T. C. (2014). SETD2-Dependent Histone H3K36 Trimethylation Is Required for Homologous Recombination Repair

and Genome Stability. *Cell Reports*, *7*(6), 2006–2018. https://doi.org/10.1016/j.celrep.2014.05.026

Pfister, S. X., Markkanen, E., Jiang, Y., Sarkar, S., Woodcock, M., Orlando, G., … Humphrey, T. C. (2015). Inhibiting WEE1 Selectively Kills Histone H3K36me3-Deficient Cancers by dNTP Starvation. *Cancer Cell*, *28*(5), 557–568. https://doi.org/10.1016/j.ccell.2015.09.015

Pines, J. (1995). Cyclins and cyclin-dependent kinases: a biochemical view. *Biochemical Journal*, *308*(3), 697–711. https://doi.org/10.1042/bj3080697

Pines, J., & Hunter, T. (1989). Isolation of a human cyclin cDNA: Evidence for cyclin mRNA and protein regulation in the cell cycle and for interaction with p34cdc2. *Cell*, *58*(5), 833–846. https://doi.org/10.1016/0092-8674(89)90936-7

Poli, J., Tsaponina, O., Crabbé, L., Keszthelyi, A., Pantesco, V., Chabes, A., … Pasero, P. (2012). dNTP pools determine fork progression and origin usage under replication stress. *The EMBO Journal*, *31*(4), 883–894. https://doi.org/10.1038/emboj.2011.470

Prelich, G. (1999). Suppression mechanisms: Themes from variations. *Trends in Genetics*. https://doi.org/10.1016/S0168-9525(99)01749-7

Rebehmed, J., Revy, P., Faure, G., De Villartay, J. P., & Callebaut, I. (2014). Expanding the SRI domain family: A common scaffold for binding the phosphorylated C-terminal domain of RNA polymerase II. *FEBS Letters*, *588*(23), 4431–4437. https://doi.org/10.1016/j.febslet.2014.10.014

Ricketts, C. J., & Linehan, W. M. (2014). Intratumoral heterogeneity in kidney cancer. *Nature Genetics*, *46*(3), 214–5. https://doi.org/10.1038/ng.2904

Ruthenburg, A. J., Li, H., Patel, D. J., & David Allis, C. (2007). Multivalent engagement of chromatin modifications by linked binding modules. *Nature Reviews Molecular Cell Biology*, *8*(12), 983–994. https://doi.org/10.1038/nrm2298

Sajesh, B. V., Guppy, B. J., & McManus, K. J. (2013). Synthetic genetic targeting of genome instability in cancer. *Cancers*. https://doi.org/10.3390/cancers5030739

Sato, Y., Yoshizato, T., Shiraishi, Y., Maekawa, S., Okuno, Y., Kamura, T., … Ogawa, S. (2013). Integrated molecular analysis of clear-cell renal cell carcinoma. *Nature Genetics*, *45*(8), 860–867. https://doi.org/10.1038/ng.2699

Sen, T., Tong, P., Diao, L., Li, L., Fan, Y., Hoff, J., … Byers, L. A. (2017). *Targeting AXL and mTOR pathway overcomes primary and acquired resistance to WEE1 inhibition in small cell lung cancer*. *Clinical Cancer Research*. https://doi.org/10.1158/1078-0432.CCR-17-1284

Sherr, C. J., & Roberts, J. M. (1995). Inhibitors of mammalian G1 cyclin-dependent kinases. *Genes and Development*. https://doi.org/10.1101/gad.9.10.1149

Shilatifard, A. (2006). Chromatin Modifications by Methylation and Ubiquitination : Implications in the Regulation of Gene Expression. *Gene Expression*, *75*, 243–272. https://doi.org/10.1146/annurev.biochem.75.103004.142422

Shimura, T., Torres, M. J., Martin, M. M., Rao, V. A., Pommier, Y., Katsura, M., … Aladjem, M. I. (2008). Bloom's Syndrome Helicase and Mus81 are Required to Induce Transient Double-strand DNA Breaks in Response to DNA Replication Stress. *Journal of Molecular Biology*, *375*(4), 1152–1164. https://doi.org/10.1016/j.jmb.2007.11.006

Simons, M., Gordon, E., & Claesson-Welsh, L. (2016). Mechanisms and regulation of endothelial VEGF receptor signalling. *Nature Reviews Molecular Cell Biology*, *17*(10), 611–625. https://doi.org/10.1038/nrm.2016.87

Slaby, O., Jancovicova, J., Lakomy, R., Svoboda, M., Poprach, A., Fabian, P., … Vyzula, R. (2010). Expression of miRNA-106b in conventional renal cell carcinoma is a potential marker for prediction of early metastasis after nephrectomy. *Journal of Experimental & Clinical Cancer Research : CR*, *29*, 90. https://doi.org/10.1186/1756-9966-29-90

Smith, B. C., & Denu, J. M. (2009). Chemical mechanisms of histone lysine and arginine modifications. *Biochimica et Biophysica Acta - Gene Regulatory Mechanisms*. https://doi.org/10.1016/j.bbagrm.2008.06.005

Sorenson, M. R., Jha, D. K., Ucles, S. a, Flood, D. M., Strahl, B. D., Stevens, S. W., & Kress, T. L. (2016). Histone H3K36 methylation regulates pre-mRNA splicing in Saccharomyces cerevisiae. *RNA Biology*, *9303*(May), 1–34. https://doi.org/10.1080/15476286.2016.1144009

Strahl, B. D., Grant, P. A., Briggs, S. D., Sun, Z.-W., Bone, J. R., Caldwell, J. A., … Allis, C. D. (2002). Set2 Is a Nucleosomal Histone H3-Selective Methyltransferase That Mediates Transcriptional Repression.

Molecular and Cellular Biology, *22*(5), 1298–1306. https://doi.org/10.1128/MCB.22.5.1298-1306.2002

Sudol, M., Sliwa, K., & Russo, T. (2001). Functions of WW domains in the nucleus. *FEBS Letters*. https://doi.org/10.1016/S0014-5793(01)02122-6

Sun, X. J., Wei, J., Wu, X. Y., Hu, M., Wang, L., Wang, H. H., … Chen, Z. (2005). Identification and characterization of a novel human histone H3 lysine 36-specific methyltransferase. *J Biol Chem*, *280*(42), 35261–35271. https://doi.org/M504012200 [pii] 10.1074/jbc.M504012200

Suzuki, A., Tsutomi, Y., Akahane, K., Araki, T., & Miura, M. (1998). Resistance to Fas-mediated apoptosis: activation of caspase 3 is regulated by cell cycle regulator p21WAF1 and IAP gene family ILP. *Oncogene*, *17*(8), 931–9. https://doi.org/10.1038/sj.onc.1202021

Suzuki, a, Tsutomi, Y., Miura, M., & Akahane, K. (1999). Caspase 3 inactivation to suppress Fas-mediated apoptosis: identification of binding domain with p21 and ILP and inactivation machinery by p21. *Oncogene*, *18*(5), 1239–1244. https://doi.org/10.1038/sj.onc.1202409

Taylor, S. S., & McKeon, F. (1997). Kinetochore localization of murine Bub1 is required for normal mitotic timing and checkpoint response to spindle damage. *Cell*, *89*(5), 727–735. https://doi.org/10.1016/S0092-8674(00)80255-X

Thoenes, W., Störkel, S., & Rumpelt, H. J. (1986). Histopathology and classification of renal cell tumors (adenomas, oncocytomas and carcinomas). The basic cytological and histopathological elements and their use for diagnostics. *Pathology, Research and Practice*, *181*(2), 125–143. https://doi.org/10.1016/S0344-0338(86)80001-2

Tiedemann, R. L., Hlady, R. A., Hanavan, P. D., Lake, D. F., Tibes, R., Lee, J.-H., … Robertson, K. D. (2016). Dynamic reprogramming of DNA methylation in SETD2-deregulated renal cell carcinoma. *Oncotarget*, *7*(2), 1927–46. https://doi.org/10.18632/oncotarget.6481

van den Heuvel, S., & Harlow, E. (1993). Distinct roles for cyclin-dependent kinases in cell cycle control. *Science (New York, N.Y.)*, *262*(5142), 2050–4. https://doi.org/10.1126/science.8266103

Whitfield, M. L. (2002). Identification of Genes Periodically Expressed in the Human Cell Cycle and Their Expression in Tumors. *Molecular Biology of the Cell*, *13*(6), 1977–2000. https://doi.org/10.1091/mbc.02-02-0030.

Wiedemeyer, W. R., Dunn, I. F., Quayle, S. N., Zhang, J., Chheda, M. G., Dunn, G. P., … Chin, L. (2010). Pattern of retinoblastoma pathway inactivation dictates response to CDK4/6 inhibition in GBM. *Proceedings of the National Academy of Sciences*, *107*(25), 11501–11506. https://doi.org/10.1073/pnas.1001613107

Xiang, W., He, J., Huang, C., Chen, L., Tao, D., Wu, X., … Jiang, G. (2015). miR-106b-5p targets tumor suppressor gene SETD2 to inactive its function in clear cell renal cell carcinoma. *Oncotarget*, *6*(6), 4066–4079. https://doi.org/10.18632/oncotarget.2926

Xu, J., Chen, Y., Huo, D., Khramtsov, A., Khramtsova, G., Zhang, C., … Olopade, O. I. (2016). β-catenin regulates c-Myc and CDKN1A expression in breast cancer cells. *Molecular Carcinogenesis*, *55*(5), 431–439. https://doi.org/10.1002/mc.22292

Yanagida, M. (2000). Cell cycle mechanisms of sister chromatid separation; roles of Cut1/separin and Cut2/securin. *Genes to Cells : Devoted to Molecular & Cellular Mechanisms*, *5*(1), 1–8. https://doi.org/gtc306 [pii]

Yi, X., Tao, Y., Lin, X., Dai, Y., Yang, T., Yue, X., … Chang, J. (2017). Histone methyltransferase Setd2 is critical for the proliferation and differentiation of myoblasts. *Biochimica et Biophysica Acta - Molecular Cell Research*, *1864*(4), 697–707. https://doi.org/10.1016/j.bbamcr.2017.01.012

Yoh, S. M., Lucas, J. S., & Jones, K. A. (2008). The Iws1:Spt6:CTD complex controls cotranscriptional mRNA biosynthesis and HYPB/Setd2-mediated histone H3K36 methylation. *Genes and Development*, *22*(24), 3422–3434. https://doi.org/10.1101/gad.1720008

Zeman, M. K., & Cimprich, K. A. (2014). Causes and consequences of replication stress. *Nature Cell Biology*, *16*(1), 2–9. https://doi.org/10.1038/ncb2897

Zhang, X., Yalcin, S., Lee, D.-F., Yeh, T.-Y. J., Lee, S.-M., Su, J., … Ghaffari, S. (2011). FOXO1 is an essential regulator of pluripotency in human embryonic stem cells. *Nature Cell Biology*, *13*(9), 1092–1099. https://doi.org/10.1038/ncb2293

Zhou, B. P., Liao, Y., Xia, W., Spohn, B., Lee, M. H., & Hung, M. C. (2001). Cytoplasmic localization of p21Cip1/WAF1 by Akt-induced phosphorylation in HER-2/neu-overexpressing cells. *Nature Cell Biology*, *3*(3), 245–252. https://doi.org/10.1038/35060032